

Forecasting range shifts of a dioecious plant species under climate change

Jacob K. Moutouama 0000-0003-1599-1671^{*1}, Aldo Compagnoni 0000-0001-8302-7492², and Tom E.X. Miller 0000-0003-3208-6067¹

¹Program in Ecology and Evolutionary Biology, Department of BioSciences, Rice University, Houston, Texas, USA

²Institute

of Biology, Martin Luther University Halle-Wittenberg, Halle, Germany; and German Centre for Integrative Biodiversity Research (iDiv), Leipzig, Germany

Running header: Forecasting range shifts

Keywords: demography, forecasting, global warming, matrix projection model, population dynamics, sex ratio, range limits

Submitted to: *Ecology letters* (Letter)

Data accessibility statement: All data used in this paper are publicly available and cited appropriately (Miller and Compagnoni, 2022a). Should the paper be accepted, all computer scripts supporting the results will be archived in a Zenodo package, with the DOI included at the end of the article. During peer review, our code (Stan and R) is available at <https://github.com/jmoutouama/POAR-Forecasting>.

Conflict of interest statement: None.

Authorship statement: J.K.M., A.C. and T.E.X.M. designed the study. A.C. and T.E.X.M. collected the data. All authors conducted the statistical analyses and modeling. J.K.M. drafted the manuscript, and T.E.X.M contributed to revisions.

Abstract:

Main Text:

Figures: 6

Tables: 0

References: 106

*Corresponding author: jmoutouama@gmail.com

¹ Abstract

² Global warming has triggered an urgent need for predicting the reorganization of Earth's
³ biodiversity. Currently, the majority of models used to forecast population viability and range
⁴ shifts in response to climate change ignore the the complication of sex structure, and thus the
⁵ potential for females and males to differ in their sensitivity to climate drivers. We developed
⁶ demographic models of range limitation, parameterized from geographically distributed
⁷ common garden experiments, with females and males of a dioecious grass species (*Poa*
⁸ *arachnifera*) throughout and beyond its range in the south-central U.S. Female-dominant and
⁹ two-sex model versions both predict that climate change will alter population viability and
¹⁰ will induce a poleward niche shift beyond current northern limits. However, the magnitude of
¹¹ niche shift was underestimated by the female-dominant model, because females have broader
¹² temperature tolerance than males and become mate-limited under female-biased sex ratios.
¹³ Our result illustrate how explicit accounting for both sexes could enhance population viability
¹⁴ forecasts and conservation planning for dioecious species in response to climate change.

15 **Introduction**

16 Rising temperatures and extreme drought events associated with global climate change are
17 leading to increased concern about how species will become redistributed across the globe
18 under future climate conditions (Bertrand et al., 2011; Gamelon et al., 2017; Smith et al., 2024).
19 Species' range limits, when not driven by dispersal limitation, should generally reflect the limits
20 of the ecological niche (Lee-Yaw et al., 2016). Niches and geographic ranges are often limited
21 by climatic factors including temperature and precipitation (Sexton et al., 2009). Therefore,
22 any substantial changes in the magnitude of these climatic factors could impact population
23 viability, with implications for range expansions or contractions based on which regions of
24 a species' range become more or less suitable (Davis and Shaw, 2001; Pease et al., 1989).

25 Forecasting range shifts for dioecious species (most animals and ca. 7% of plant species)
26 is complicated by the potential for sexual niche differentiation, i.e. distinct responses of
27 females and males to shared climate drivers (Hultine et al., 2016; Morrison et al., 2016; Pottier
28 et al., 2021; Tognetti, 2012). For instance, the lower cost of reproduction for one sex (male or
29 female) may allow that sex to invest its energy toward other functions that result in higher
30 growth rates, greater clonality, or even improved survival rates compared to the other sex,
31 leading to sexual niche differentiation (Bruijning et al., 2017).¹ Accounting for sexual niche
32 differentiation is a long-standing challenge in accurately predicting which sex will successfully
33 track environmental change and how this will impact population viability and range shifts
34 (Gissi et al., 2023; Jones et al., 1999). Populations in which males are rare under current climatic
35 conditions could experience low reproductive success due to sperm or pollen limitation that
36 may lead to population decline in response to climate change that disproportionately favors
37 females (Eberhart-Phillips et al., 2017). In contrast, climate change could expand male habitat
38 suitability (e.g. upslope movement), which might increase seed set for mate-limited females
39 and favor range expansion (Petry et al., 2016). Across dioecious plants, for example, studies
40 suggest that future climate change toward hotter and drier conditions may favor male-biased
41 sex ratios (Field et al., 2013; Hultine et al., 2016). Although the response of species to climate
42 warming is an urgent and active area of research, few studies have disentangled the interaction
43 between sex and climate drivers to understand their combined effects on population dynamics
44 and range shifts, despite calls for such an approach (Gissi et al., 2023; Hultine et al., 2016).

45 The vast majority of theory and models in population biology, including those used
46 to forecast biodiversity responses to climate change, ignore the complication of sex structure
47 (but see Ellis et al., 2017; Gissi et al., 2024; Pottier et al., 2021). Traditional approaches instead

¹I added this to talk about the cost of reproduction explaining niche differentiation as you suggested

48 focus exclusively on females, assuming that males are in sufficient supply as to never limit
49 female fertility. In contrast, “two-sex” models are required to fully account for demographic
50 differences between females and males and sex-specific responses to shared climate drivers
51 (Gerber and White, 2014; Miller et al., 2011). Sex differences in maturation, reproduction,
52 and mortality schedules can generate skew in the operational sex ratio (OSR; sex ratio of
53 individuals available for mating) even if the birth sex ratio is 1:1 (Eberhart-Phillips et al., 2017;
54 Shelton, 2010). Climate and other environmental drivers can therefore influence the OSR
55 via their influence on sex-specific demographic rates. In a two-sex framework, demographic
56 rates both influence and respond to the OSR in a feedback loop that makes two-sex models
57 inherently nonlinear and more data-hungry than corresponding female-dominant models.
58 Given the additional complexity and data needs, forecasts of range dynamics for dioecious
59 species under future climate change that explicitly account for females, males, and their
60 inter-dependence are limited (Lynch et al., 2014; Petry et al., 2016).

61 Tracking the impact of climate change on population viability (λ) and distributional
62 limits of dioecious taxa depends on our ability to build mechanistic models that take into
63 account the spatial and temporal context of sex specific response to climate change, while
64 accounting for sources of uncertainty (Davis and Shaw, 2001; Evans et al., 2016). Structured
65 population models built from demographic data collected from geographically distributed
66 observations or common garden experiments provide several advantages for studying
67 the impact of climate change on species’ range shifts (Merow et al., 2017; Schultz et al.,
68 2022; Schwinning et al., 2022). First, demographic models link individual-level life history
69 events (mortality, development, and regeneration) to population demography, allowing the
70 investigation of factors explaining vital rate responses to environmental drivers (Dahlgren
71 et al., 2016; Ehrlén and Morris, 2015; Louthan et al., 2022). Second, demographic models
72 have a natural interface with statistical estimation of individual-level vital rates that provide
73 quantitative measures of uncertainty and isolate different sources of variation, features that
74 can be propagated to population-level predictions (Elderd and Miller, 2016; Ellner et al.,
75 2022). Finally, structured demographic models can be used to identify which aspects of
76 climate are the most important drivers of population dynamics. For example, Life Table
77 Response Experiments (LTRE) built from structured models have become widely used to
78 understand the relative importance of covariates in explaining variation in population growth
79 rate (Czachura and Miller, 2020; Ellner et al., 2016; Hernández et al., 2023).

80 In this study, we combined geographically-distributed common garden experiments,
81 hierarchical Bayesian statistical modeling, two-sex population projection modeling, and climate
82 back-casting and forecasting to understand demographic responses to climate change and their
83 implications for past, present, and future range dynamics. Our work focused on the dioecious

84 plant Texas bluegrass (*Poa arachnifera*), which is distributed along environmental gradients
85 in the south-central U.S. corresponding to variation in temperature across latitude and
86 precipitation across longitude (Fig. S-1A)². This region has experienced rapid climate warming
87 since 1900 and this is projected to continue through the end of the century (Fig. 1). Our
88 previous study showed that, despite evidence for differentiation of climatic niche between sexes,
89 the female niche mattered the most in driving longitudinal range limits of Texas bluegrass
90 (Miller and Compagnoni, 2022b). However, that study used a single proxy variable (longitude)
91 to represent environmental variation related to aridity and did not consider variation in
92 temperature, which is the much stronger dimension of forecasted climate change in this region
93 (Fig. S-3). Developing a rigorous forecast for the implications of future climate change requires
94 that we transition from implicit to explicit treatment of multiple climate drivers, as we do
95 here. Leveraging the power of Bayesian inference, we take a probabilistic view of past, present,
96 and future range limits by quantifying the probability of population viability ($Pr(\lambda \geq 1)$) in
97 relation to climate drivers of demography, an approach that fully accounts for uncertainty
98 arising from multiple sources of estimation and process error. Specifically, we asked:

- 99 1. What are the sex-specific vital rate responses to variation in temperature and precipitation
100 across the species' range?
- 101 2. How do sex-specific vital rates combine to determine the influence of climate variation
102 on population growth rate (λ)?
- 103 3. What is the impact of climate change on operational sex ratio throughout the range?
- 104 4. What are the likely historical and projected dynamics of the Texas bluegrass geographic
105 niche and how does accounting for sex structure modify these predictions?

106 Materials and methods

107 Study species and climate context

108 Texas bluegrass (*Poa arachnifera*) is a dioecious perennial, summer-dormant cool-season (C3)
109 grass that occurs in the south-central U.S. (Texas, Oklahoma, and southern Kansas) (Figure
110 1) (Hitchcock, 1971). Texas bluegrass grows between October and May, flowers in spring,
111 and goes dormant during the hot summer months of June to September (Kindiger, 2004).
112 Following this life history, we divided the calendar year into growing (October 1 - May
113 31) and dormant (June 1 - September 30) seasons in the analyses below. Biological sex is
114 genetically based and the birth (seed) sex ratio is 1:1 (Renganayaki et al., 2005). Females and

²I added this Figure because it its the best one illustrating what we are saying here

¹¹⁵ males are morphologically indistinguishable except for their inflorescences. Like all grasses,
¹¹⁶ this species is wind pollinated (Hitchcock, 1971) and most male-female pollen transfer occurs
¹¹⁷ within 10-15m (Compagnoni et al., 2017). Surveys of 22 natural populations throughout the
¹¹⁸ species' distribution indicated that operational sex ratio (the female fraction of inflorescences)
¹¹⁹ ranged from 0.007 to 0.986 with a mean of 0.404 (Miller and Compagnoni, 2022b).

¹²⁰ Latitudinal limits of the Texas bluegrass distribution span 7.74 °C to 16.94 °C of
¹²¹ temperature during the dormant season and 24.38 °C to 28.80 °C during the dormant season.
¹²² Longitudinal limits span 244.9 mm to 901.5 mm of precipitation during the growing season
¹²³ and 156.3 mm to 373.3 mm. This region has experienced *ca.* 0.5 °C of climate warming since
¹²⁴ 1900, with faster warming during the cool-season months (0.0055°C/yr) than the hot summers
¹²⁵ (0.0046°C/yr) (Fig. S-2). Future warming is projected to accelerate to 0.03 – 0.06°C/yr by
¹²⁶ the end of the century depending on the season and forecast model. On the other hand,
¹²⁷ precipitation has increased over the past century for much of the region but is forecasted
¹²⁸ to decline back to early-20th century levels (Fig. S-2).

¹²⁹ Common garden experiment

¹³⁰ Experimental design

¹³¹ We conducted a range-wide common garden experiment to quantify sex-specific demographic
¹³² responses to climate variation. Details of the experimental design are provided in Miller
¹³³ and Compagnoni (2022b); we provide a brief overview here. The experiment was installed
¹³⁴ at 14 sites throughout and, in some cases, beyond the natural range of Texas bluegrass that
¹³⁵ sampled a broad range of latitude and longitude (Figure 1A). At each site, we established
¹³⁶ 14 blocks. For each block we planted three female and three male individuals that were
¹³⁷ clonally propagated from females and males from eight natural source populations (Figure
¹³⁸ 1A); because sex is genetically-based, clones never deviated from their expected sex. The
¹³⁹ experiment was established in November 2013 with a total of 588 female and 588 male plants,
¹⁴⁰ and was censused in May of 2014, 2015, and 2016. At each census, we collected data on
¹⁴¹ survival, size (number of tillers), and number of panicles (reproductive inflorescences). For
¹⁴² the analyses that follow, we focus on the 2014-15 and 2015-16 transition years, since the start
¹⁴³ of the experiment did not include the full 2013-14 transition year.

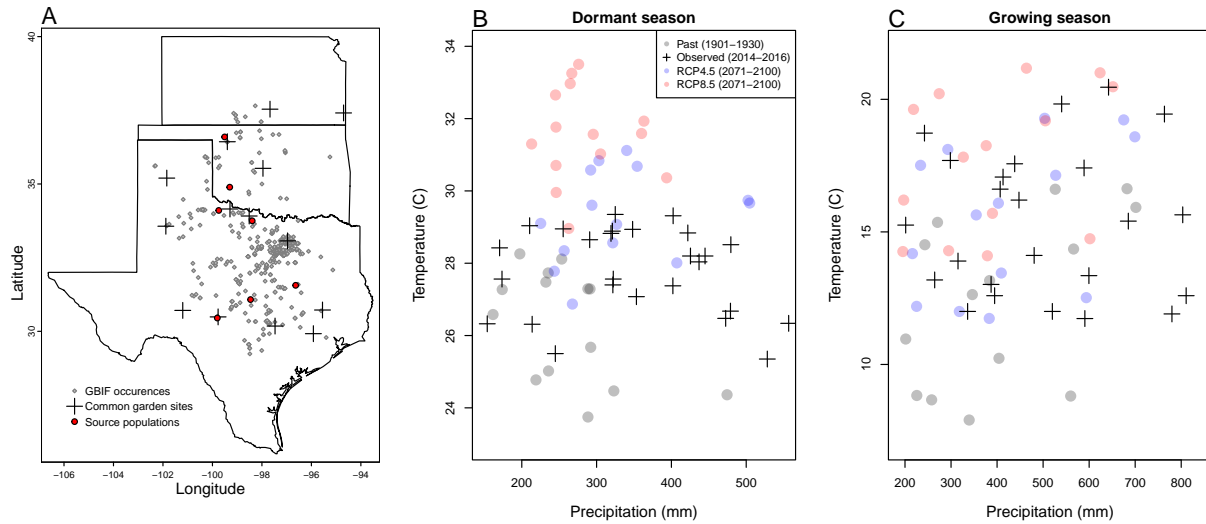


Figure 1: Experimental gardens and climate of the study region. **A:** Map of 14 experimental garden sites (crosses) in Texas, Oklahoma, and Kansas relative to GBIF occurrences of *Poa arachnifera* (gray points). Red points indicate source populations for plants used in the common garden experiment. **B,C:** Past, future, and observed climate space for growing and dormant seasons. Crosses show observed conditions for the sites and years of the common garden experiment. Gray points show historical (1901-1930) climate normals, and blue and red points show end-of-century (2071-2100) climate normals for RCP4.5 and RCP8.5 projections, respectively, from MIROC5.

144 Climatic data collection

145 We gathered downscaled monthly temperature and precipitation for each site from Chelsa
 146 (Karger et al., 2017) to describe observed climate conditions during our study period. These
 147 climate data were used as covariates in vital rate regressions. We aligned the climatic years
 148 to match demographic transition years (June 1 – May 31) and growing and dormant seasons
 149 within each year. To back-cast and forecast demographic responses to changes in climate
 150 throughout the study region, we also gathered projection data for three 30-year periods: “past”
 151 (1901-1930), “current” (1990-2019) and “future” (2070-2100). Data for future climatic periods
 152 were downloaded from four general circulation models (GCMs) selected from the Coupled
 153 Model Intercomparison Project Phase 5 (CMIP5): Model for Interdisciplinary Research on
 154 Climate (MIROC5), Australian Community Climate and Earth System Simulator (ACCESS1-3),
 155 Community Earth System Model (CESM1-BGC), Centro Euro-Mediterraneo sui Cambiamenti
 156 Climatici Climate Model (CMCC-CM). All the GCMs were also downloaded from Chelsa
 157 (Sanderson et al., 2015). We evaluated future climate projections from two scenarios of
 158 representative concentration pathways (RCPs): RCP4.5, an intermediate-to-pessimistic scenario
 159 assuming a radiative forcing amounting to 4.5 W m^{-2} by 2100, and RCP8.5, a pessimistic

¹⁶⁰ emission scenario which projects a radiative forcing of 8.5 Wm^{-2} by 2100 (Schwalm et al.,
¹⁶¹ 2020; Thomson et al., 2011).

¹⁶² Projection data for the three 30-year periods included warmer or colder conditions than ob-
¹⁶³ served in our experiment, so extending our inferences to these conditions required some extrap-
¹⁶⁴ olation. However, across all sites, both study years were 1–2°C warmer than their correspond-
¹⁶⁵ ing “current” (1990–2019) temperature normals (Fig. S-3). Additionally, the 2014–15 growing
¹⁶⁶ season was generally wetter and cooler across the study region than 2015–16 (Fig. S-3). Com-
¹⁶⁷ bined, the geographic and inter-annual replication of the common garden experiment provided
¹⁶⁸ good coverage of most past and future conditions throughout the study region (Fig. 1B,C).

¹⁶⁹ **Sex-specific demographic responses to climatic variation across common garden sites**

¹⁷⁰ We used individual-level measurements of survival, growth (change in number of tillers),
¹⁷¹ flowering, and number of panicles (conditional on flowering) to develop Bayesian mixed
¹⁷² effect models describing how each vital rate varies as a function of sex, size, and four climate
¹⁷³ covariates (precipitation and temperature of growing and dormant season). These vital rate
¹⁷⁴ models included main effects of size (the natural log of tiller number), sex, and seasonal
¹⁷⁵ climate covariates (Supplementary Method S.2.1).

¹⁷⁶ **Sex ratio responses to climatic variation across common garden sites**

¹⁷⁷ We also used the experimental data to investigate how climatic variation across the range
¹⁷⁸ influenced sex ratio and operational sex ratio of the common garden populations. To do so,
¹⁷⁹ we developed two Bayesian linear models using data collected during three years. Each model
¹⁸⁰ had OSR or SR as response variable and a climate variable (temperature and precipitation
¹⁸¹ of the growing season and dormant season) as predictor (Supplementary Method S.2.2).

¹⁸² **Model-fitting procedures**

¹⁸³ All models were fit using Stan (Stan Development Team, 2023) in R 4.3.1 (R Core Team,
¹⁸⁴ 2023). We centered and standardized all climatic predictors to mean zero, variance one, which
¹⁸⁵ facilitated model convergence. We ran three chains for 1000 samples for warmup and 4000
¹⁸⁶ for sampling, with a thinning rate of 3. We assessed the quality of the models using posterior
¹⁸⁷ predictive checks (Piironen and Vehtari, 2017) (Fig. S-4).

188 **Two-sex and female-dominant matrix projection models**

189 We used the climate-dependent vital rate regressions estimated above, combined with
 190 additional data sources, to build female-dominant and two-sex versions of a climate-explicit
 191 matrix projection model (MPMs) structured by the discrete state variables size (number
 192 of tillers) and sex. The female-dominant and two-sex versions of the model both allow
 193 for sex-specific response to climate and differ only in the feedback between operational
 194 sex ratio and seed fertilization. For clarity of presentation we do not explicitly include
 195 climate-dependence in the notation below, but the following model was evaluated over
 196 variation in seasonal temperature and precipitation.

197 Let $F_{x,t}$ and $M_{x,t}$ be the number of female and male plants of size x in year t , where
 198 $x \in [1, \dots, U]$. The minimum possible size is one tiller and U is the 95th percentile of observed
 199 maximum size (35 tillers). Let F_t^R and M_t^R be new female and male recruits in year t , which
 200 we treat as distinct from the rest of the size distribution because we assume they do not
 201 reproduce in their first year, consistent with our observations. For a pre-breeding census,
 202 the expected numbers of recruits in year $t+1$ is given by:

$$203 \quad F_{t+1}^R = \sum_1^U [p^F(x) \cdot c^F(x) \cdot d \cdot v(\mathbf{F}_t, \mathbf{M}_t) \cdot m \cdot \rho] F_{x,t} \quad (1)$$

$$204 \quad M_{t+1}^R = \sum_1^U [p^F(x) \cdot c^F(x) \cdot d \cdot v(\mathbf{F}_t, \mathbf{M}_t) \cdot m \cdot (1-\rho)] F_{x,t} \quad (2)$$

205 where p^F and c^F are flowering probability and panicle production for females of size x , d
 206 is the number of seeds per female panicle, v is the probability that a seed is fertilized, m is
 207 the probability that a fertilized seed germinates, and ρ is the primary sex ratio (proportion
 208 of recruits that are female), which we assume to be 0.5 (Miller and Compagnoni, 2022b).

209 In the two-sex model, seed fertilization is a function of population structure, allowing for
 210 feedback between vital rates and operational sex ratio (OSR). In the context of the model, OSR
 211 is defined as the fraction of panicles that are female and is derived from the $U \times 1$ vectors
 212 \mathbf{F}_t and \mathbf{M}_t :

$$213 \quad v(\mathbf{F}_t, \mathbf{M}_t) = v_0 * \left[1 - \left(\frac{\sum_1^U p^F(x, z) c^F(x, z) F_{x,t}}{\sum_1^U p^F(x, z) c^F(x, z) F_{x,t} + p^M(x, z) c^M(x, z) M_{x,t}} \right)^\alpha \right] \quad (3)$$

214 The summations tally the total number of female and male panicles over the size distribution,
 215 giving the fraction of total panicles that are female. We focus on the female fraction of
 216 panicles and not female fraction of reproductive individuals because panicle number can vary
 217 widely depending on size; we assume that few males with many panicles vs. many males

218 with few panicles are interchangeable pollination environments. Eq. 3 has the properties
 219 that seed fertilization is maximized at v_0 as OSR approaches 100% male, goes to zero as OSR
 220 approaches 100% female, and parameter α controls how female seed viability declines as male
 221 panicles become rare. We estimated these parameters using data from a sex ratio manipulation
 222 experiment, conducted in the center of the range, in which seed fertilization was measured
 223 in plots of varying OSR; this experiment is described elsewhere (Compagnoni et al., 2017) and
 224 is summarized in **Supplementary Method S.2.3**³. This experiment also provided estimates for
 225 seed number per panicle (d) and germination rate (m). Lacking data on climate-dependence,
 226 we assume that seed fertilization, seed number, and germination rate do not vary with climate.
 227

The dynamics of the size-structured component of the population are given by:

$$F_{y,t+1} = [\sigma \cdot g^F(y, x=1)] F_t^R + \sum_L^U [s^F(x) \cdot g^F(y, x)] F_{x,t} \quad (4)$$

$$M_{y,t+1} = [\sigma \cdot g^M(y, x=1)] M_t^R + \sum_L^U [s^M(x) \cdot g^M(y, x)] M_{x,t} \quad (5)$$

230 The first terms indicate recruits that survived their first year and enter the size distribution
 231 of established plants. We estimated the seedling survival probability σ using demographic
 232 data from the congeneric species *Poa autumnalis* in east Texas (T.E.X. Miller and J.A. Rudgers,
 233 *unpublished data*), and we assume that σ is the same across sexes and climatic variables. We did
 234 this because we had little information on the early life cycle transitions of greenhouse-raised
 235 transplants. We used $g(y, x=1)$ (the future size distribution of one-tiller plants from the
 236 transplant experiment) to give the probability that a surviving recruit reaches size y . The
 237 second component of the equations indicates survival and size transition of established
 238 plants from the previous year, where s and g give the probabilities of surviving at size x and
 239 growing from sizes x to y , respectively, and superscripts indicate that these functions may
 240 be unique to females (F) and males (M).

241 The model described above yields a $2(U+1) \times 2(U+1)$ transition matrix. We estimated
 242 the population growth rate λ of the female dominant model as the leading eigenvalue of
 243 the transition matrix. Since the two-sex MPM is nonlinear (matrix elements affect and are
 244 affected by population structure) we estimated λ and stable sex ratio (female fraction of all
 245 individuals) and operational sex ratio (female fraction of panicles) by numerical simulation.
 246 Since all parameters were estimated using MCMC sampling, we were able to propagate the
 247 uncertainty in our estimates of the vital rate parameters to uncertainty in λ . Furthermore,
 248 by sampling over distributions associated with site, block, and source population variance

³I think the supplement should also include a data figure showing the fit of the model to the experimental data.

249 terms, we are able to incorporate process error into the total uncertainty in λ , in addition
250 to the uncertainty that arises from imperfect knowledge of the parameter values. For example,
251 sampling over site and block variances accounts for regional and local spatial heterogeneity
252 that is not explained by climate, and sampling over source population variance accounts for
253 genetically-based demographic differences across the species' range.

254 Life Table Response Experiments

255 We conducted two types of Life Table Response Experiments (LTRE) to isolate contributions of
256 climate variables and sex-specific vital rates to variation in λ . First, to identify which aspect of
257 climate is most important for population viability, we used an LTRE based on a nonparametric
258 model for the dependence of λ on parameters associated with seasonal temperature and
259 precipitation (Ellner et al., 2016). To do so, we used the RandomForest package to fit a
260 regression model with four climatic variables (temperature of growing season, precipitation of
261 growing season, temperature of the dormant season and precipitation of the dormant season)
262 as predictors and λ calculated from the two sex model as response (Liaw et al., 2002). The
263 regression model allowed the estimation of the relative importance of each predictor.

264 Second, to understand how climate drivers influence λ via sex-specific demography, we
265 decomposed the effect of each climate variable on population growth rate (λ) into contribution
266 arising from the effect on each female and male vital rate using a “regression design” LTRE
267 (Caswell, 1989, 2000). This LTRE decomposes the sensitivity of λ to climate according to:

$$268 \quad \frac{\partial \lambda}{\partial \text{climate}} \approx \sum_i \frac{\partial \lambda}{\partial \theta_i^F} \frac{\partial \theta_i^F}{\partial \text{climate}} + \frac{\partial \lambda}{\partial \theta_i^M} \frac{\partial \theta_i^M}{\partial \text{climate}} \quad (6)$$

269 where, θ_i^F and θ_i^M represent sex-specific parameters (the regression coefficients of the vital
270 rate functions). Because LTRE contributions are additive, we summed across vital rates to
271 compare the total contributions of female and male parameters.⁴⁵

272 Population viability across the climatic niche and geographic range

273 To understand how climate shapes the niche and geographic range of Texas bluegrass, we
274 estimated the probability of self- sustaining populations ($\Pr(\lambda \geq 1)$) conditional to temperature
275 and precipitation of the dormant and growing seasons. $\Pr(\lambda > 1)$ was calculated for the

⁴Let's talk about this

⁵I do not agree. It is true that you can compute this, but only by “turning off” the interaction by holding the interacting variable constant. I still think this needs to be better addressed in both LTRE analyses.

²⁷⁶ two-sex model and the female dominant MPMs using the proportion of the 300 posterior
²⁷⁷ samples that lead to a $\lambda \geq 1$ (Diez et al., 2014). Population viability in climate niche space
²⁷⁸ was then represented as a contour plot with values of $\text{Pr}(\lambda > 1)$ at given temperature and
²⁷⁹ precipitation for the growing season, holding dormant season climate constant, and vice versa.

²⁸⁰ $\text{Pr}(\lambda > 1)$ was also mapped onto geographic layers of three US states (Texas, Oklahoma
²⁸¹ and Kansas) to delineate past, current and future potential geographic distribution of the
²⁸² species. To do so, we estimated $\text{Pr}(\lambda > 1)$ conditional to all climate covariates for each
²⁸³ pixel ($\sim 25 \text{ km}^2$) for each time period (past, present, future). Because of the amount of the
²⁸⁴ computation involved, we use 100 posterior samples to estimate $\text{Pr}(\lambda > 1)$ across the study
²⁸⁵ area (Texas, Oklahoma and Kansas).

²⁸⁶ Results

²⁸⁷ Sex specific demographic responses and sex ratio variation across climatic ²⁸⁸ conditions

²⁸⁹ We found strong demographic responses to climate drivers across our Texas bluegrass com-
²⁹⁰ mon garden sites and years, and evidence for demographic differences between the sexes.
²⁹¹ Regression coefficients related to sex and/or sex:size interactions were significantly non-zero
²⁹² (95% credible intervals excluding zero) for most vital rates (Fig. S-5), suggesting sexual diver-
²⁹³ gence in demography. Females generally had an advantage over males, especially in survival
²⁹⁴ and flowering (Fig. 2). Furthermore, there were significant interactions between sex and one or
²⁹⁵ more climate variables, particularly for growth (Fig. S-5B), indicating sexual niche divergence
²⁹⁶ in response to shared climate drivers. Fig. S-6 and S-7 visualize the magnitude of sexual diver-
²⁹⁷ gence in demography across niche space, revealing that female advantages in flowering and
²⁹⁸ panicle production were greatest at both high and low growing season temperature extremes.

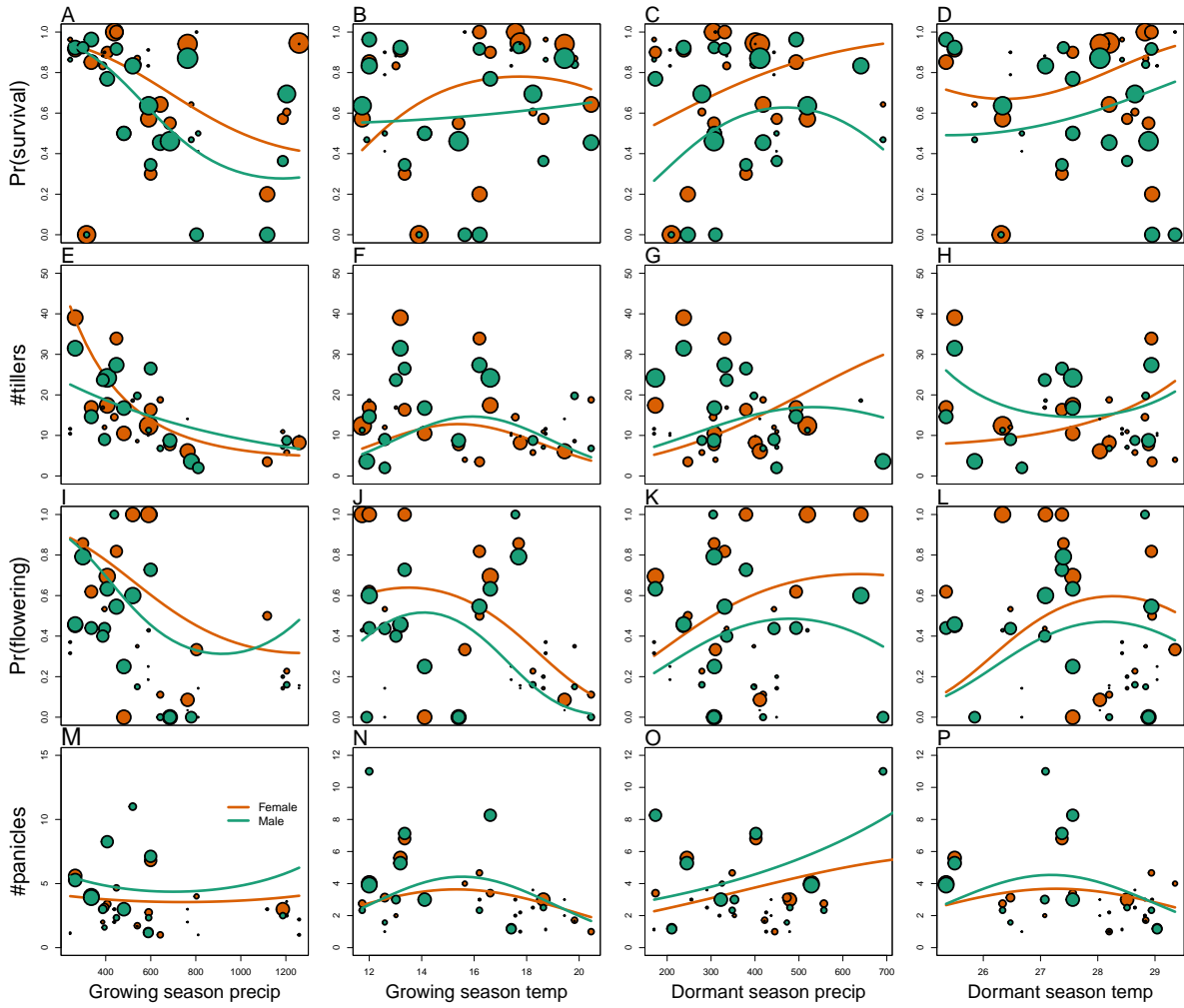


Figure 2: Sex specific demographic response to climate across species range. (A, B, C, D) Probability of survival as a function of precipitation and temperature of the growing and dormant season. (E, F, G, H) Change in number of tillers as a function of precipitation and temperature of the growing and dormant season. (I, J, K, L) Probability of flowering as a function of precipitation and temperature of growing and dormant season. (M, N, O, P) Change in number of panicles as a function of precipitation and temperature of the growing and dormant season. Points show means by site for females (orange) and males (green). Points sizes are proportional to the sample sizes of the mean and are jittered. Lines show fitted statistical models for females (orange) and males (green) based on posterior mean parameter values.

299 Across common garden sites, operational sex ratio (proportion of panicles that are female)
 300 of the experimental populations was female-biased on average ($\approx 60\%$ female), reflecting
 301 the overall greater rates of female vs. male flowering rather than bias in the underlying
 302 population composition. OSR was most female-biased (up to 80% female) at extreme values
 303 of temperature, especially growing season temperature (Fig. S-8, Fig. S-9), consistent with the
 304 female reproductive advantage at temperature extremes seen in the vital rate data (Fig. S-6). In
 305 contrast, there was very little variation in sex ratio (proportion of plants that are female) in the

306 years following common garden establishment (all sites were planted with equal numbers of
307 females and males) and no detectable influence of climate covariates (Fig. S-10), indicating that
308 skew in the OSR comes from sex-biased reproductive rates more so than sex-biased survival.

309 Climate drivers of population viability across niche space

310 Putting all vital rates together in the MPM framework reveals how climate shapes fitness
311 variation across niche dimensions and geographic space, and how accounting for sex structure
312 modifies these inferences. For both female-dominant and two-sex models, fitness variation
313 across niche space was dominated by temperature, with weaker effects of precipitation
314 (compare vertical and horizontal contours in Fig. 3). These visual trends are supported by
315 LTRE decomposition indicating that variation in fitness across climatic conditions is most
316 strongly driven by responses to growing and dormant season temperature, with weaker
317 interactive effects of precipitation that modulate the effects of temperature (Fig. S-12). LTRE
318 analysis also showed that declines in population viability at high and low temperatures were
319 driven most strongly by reductions in vegetative growth and panicle production, with stronger
320 contributions from females than males (Fig. S-13). Intermediate temperatures of both growing
321 and dormant seasons were associated with near-certain projections of population viability
322 ($Pr(\lambda \geq 1) \approx 1$), and high and low temperature extremes during both seasons were associated
323 with low niche suitability ($Pr(\lambda \geq 1) < 0.2$). Higher precipitation slightly expanded the range
324 of suitable temperatures during the dormant season (Fig. 3A), and the reverse was true in
325 the growing season (Fig. 3B). Points in Fig. 3 show that climate change forecasted for the
326 common garden locations would move many of them toward lower-suitability regions of niche
327 space associated with high growing and dormant season temperatures (see also Fig. S-14).

328 While the female-dominant and two-sex models were generally in agreement about high
329 confidence in intermediate temperature optima, they differed around the edges of niche space
330 (Fig. 3C,D,S-14). The female-dominant model over-predicted population viability, especially
331 with respect to growing season temperature. For example, the female-dominant model
332 predicted⁶ that, for most levels of precipitation, warm growing season (winter) temperatures
333 of $\sim 20^{\circ}\text{C}$ had high suitability ($Pr(\lambda \geq 1) > 0.9$), while the two-sex model indicated that these
334 conditions were most likely unsuitable ($Pr(\lambda \geq 1) < 0.5$). Similarly, at low winter temperatures
335 that the two-sex model identifies with high certainty as unsuitable ($Pr(\lambda \geq 1) < 0.1$), the
336 female-dominant model is more optimistic ($Pr(\lambda \geq 1) > 0.4$). Across growing season climate
337 space, the female-dominant model over-estimates population viability by ca. 9.23%, on
338 average (Fig. 3D, Fig. S-15B). The difference between female-dominant and two-sex models

⁶I think I am switching tenses. We will need to clean this up.

³³⁹ was qualitatively similar but weaker in magnitude for niche dimensions of the dormant
³⁴⁰ season (Fig. 3C, Fig. S-15A). Female-dominant and two-sex models diverged most strongly in
³⁴¹ regions of niche space that favored strongly female-biased operational sex ratios (Fig. S-16)⁷⁸.
³⁴² This suggests mate limitation as the biological mechanism underlying model differences.
³⁴³ The two-sex model accounts for feedbacks between OSR and female fertility, with reduced
³⁴⁴ seed viability at OSR exceeding ~ 75% female panicles (Fig. S-17) Lacking this feedback, the
³⁴⁵ female-dominant model over-predicts population viability in regions of niche space where
³⁴⁶ male flowering is not sufficient to maximize seed set.

⁷*The scale is correct. Let's talk about this*

⁸*I like it! But is the scale correct on panel A?*

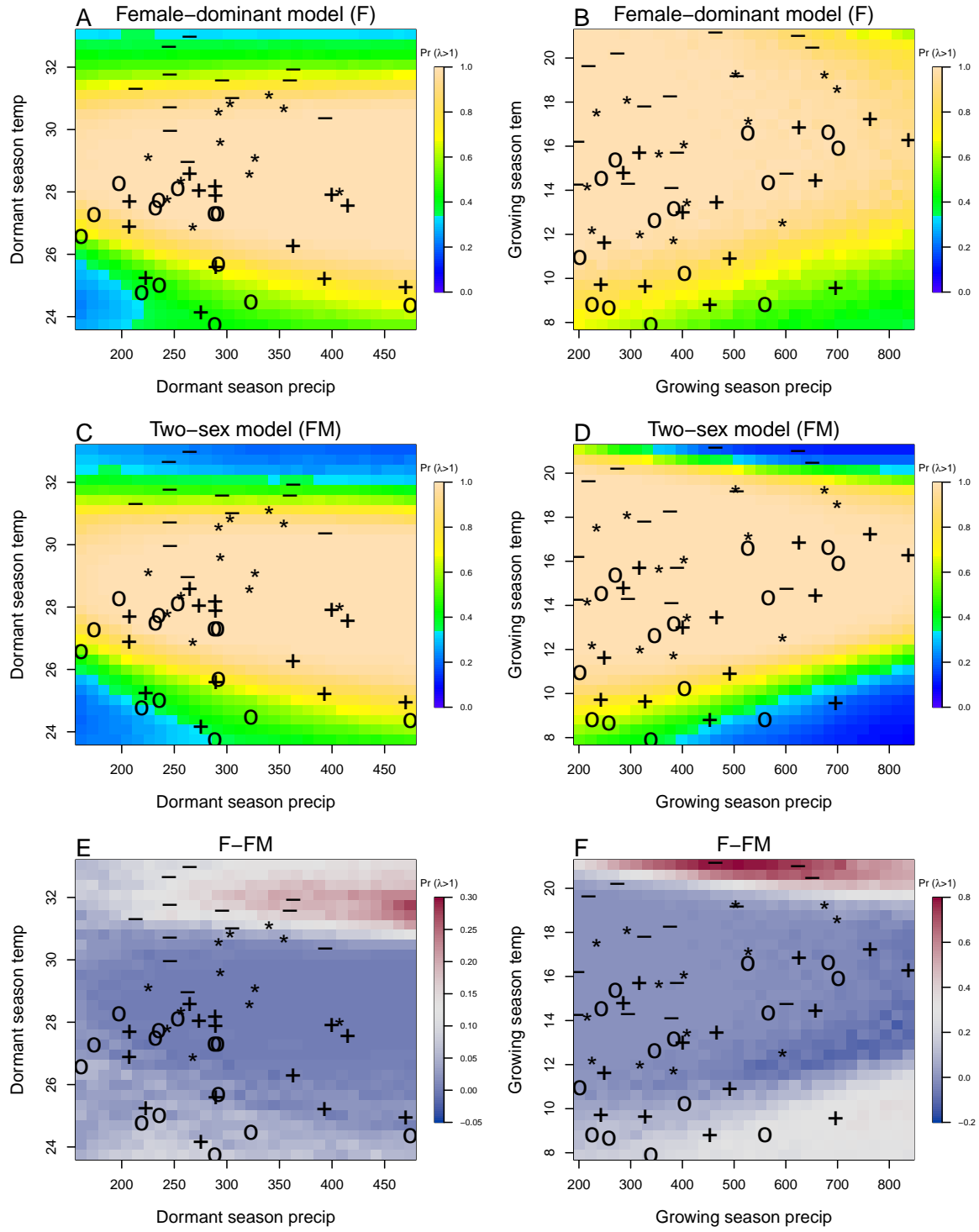


Figure 3: A two-dimensional representation of the predicted niche shift over time (past, present and future climate conditions). "O": Past, "+" Current, "*": RCP 4.5, "-": RCP 8.5.

347 **Climatic change induces shifts in geographic niche and population OSR**

348 Projecting the climatic niche onto geographic space, we find that suitable niche conditions for
349 Texas bluegrass are shifting north under climate change (Fig. 4). Under past (1901-1930) and
350 present (1990-2019) conditions, the two-sex and female-dominant models predict widespread
351 suitability with high confidence ($Pr(\lambda \geq 1) \approx 1$) across much of Texas and Oklahoma. For
352 both models, the predicted geographic niche generally corresponds well to independent ob-
353 servations of the Texas bluegrass distribution (Fig. 4). The predicted geographic niche is more
354 expansive than the GBIF occurrences, particularly at southern, western, and eastern edges, sug-
355 gesting some degree of range disequilibrium (e.g., due to dispersal limitation), geographic bias
356 in occurrence records, and/or model mis-specification. Comparing past to present conditions,
357 the geographic niche for both models has shifted slightly poleward, with reductions in viability
358 at the southern margins and expansions of viability at northern margins. The northward shift
359 of suitable niche conditions is even more pronounced in projections to end-of-century (2071-
360 2100) conditions, with the most dramatic changes in the most pessimistic (RCP8.5) scenario
361 (Fig. 4). In fact, under the pessimistic scenario, Texas bluegrass will have very little remaining
362 climate suitability in the state of Texas by the end of the 21st century. The predicted poleward
363 niche shift is consistent across different global circulation models (Fig. S-22, Fig. S-23, Fig. S-24).

364 Female-dominant and two-sex models are in broad agreement about northward
365 migration of the climatic niche, but the geographic projections reveal hotspots of disagreement
366 where the female-dominant model over-predicts climate suitability and under-predicts the
367 likelihood of range shifts (Fig. 4). These hotspots are generally regions of predicted female
368 bias in the operational sex ratio (Fig. S-18). The strongest contrast between the two models
369 is in the pessimistic climate change scenario (RCP8.5), where the female-dominant model
370 over-predicts population viability by as much as 20% across much of the region (Fig. S-25) and
371 thus under-estimates the magnitude of a potential range shift. In this scenario, a broad swath
372 of the current distribution that is forecasted to be effectively unsuitable ($Pr(\lambda \geq 1) \approx 0$) by the
373 two-sex model is identified as marginally suitable ($Pr(\lambda \geq 1) \approx 0.5$) by the female-dominant
374 model. Accordingly, the OSR of Texas bluegrass across its range is projected to be ca. 75%
375 female panicles, on average, by end of century under RCP8.5, an increase from ca. 60% female
376 under projections for past and current conditions (Fig. 5). The more optimistic climate change
377 scenario (RCP4.5) predicts an intermediate shift in OSR, with hotspots of change at northern
378 and southern range edges becoming strongly female-biased but most of the range remaining
379 near current levels of 60% female (Fig. 5; Fig. S-21, Fig. S-19, Fig. S-20).

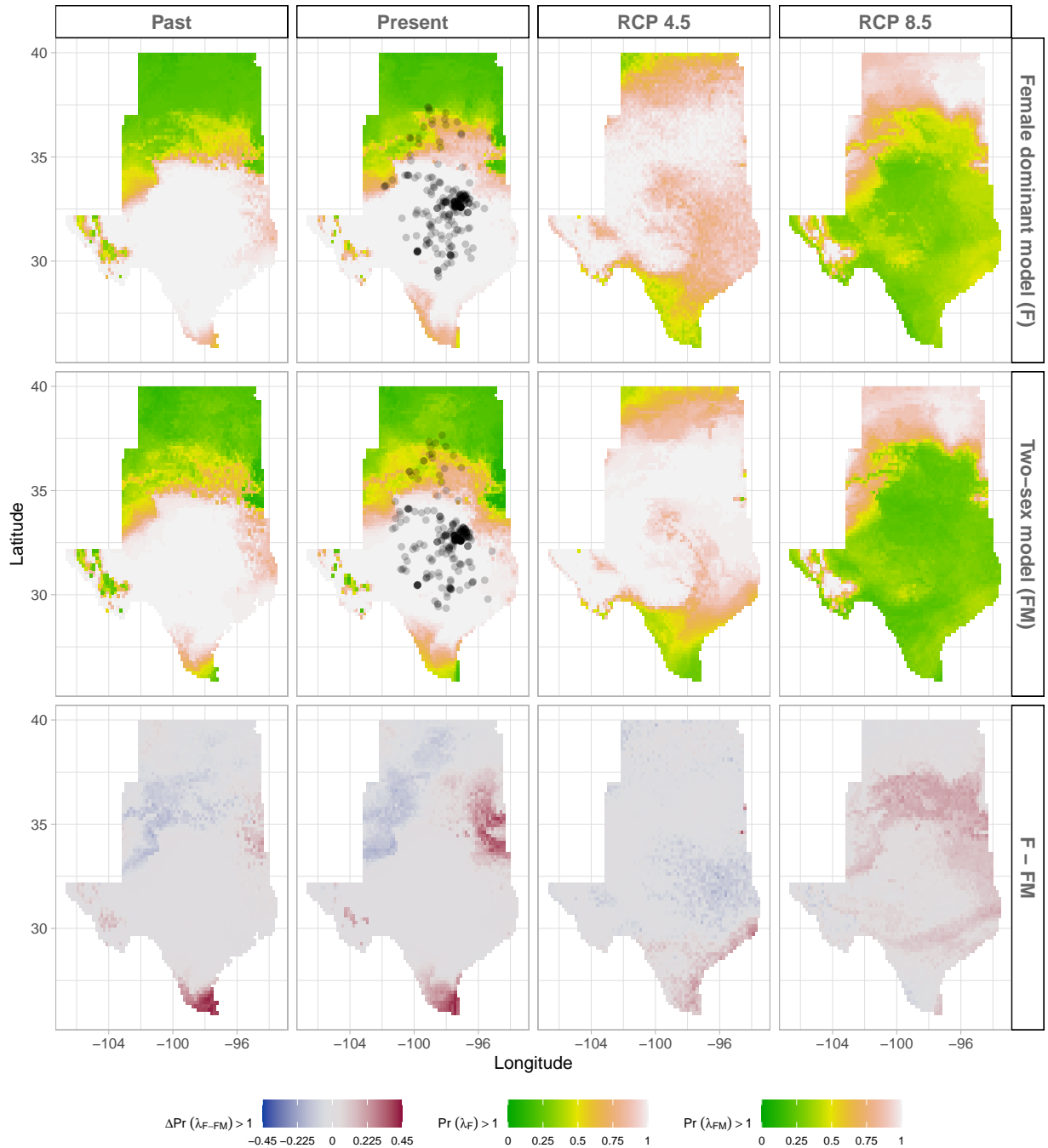


Figure 4: Climate change favors range shift towards north edge. (A) Past, (B) Current, (C and D) Future predicted range shift based on the predicted probabilities of self- sustaining populations, $\text{Pr}(\lambda > 1)$, using the two-sex model that incorporates sex- specific demographic responses to climate with sex ratio dependent seed fertilization. (E) Past, (F) Current, (G and H) Future predicted range shift based on the predicted probabilities of self- sustaining populations, $\text{Pr}(\lambda > 1)$, using the female dominant model. Future projections were based on the CMCC-CM model. The black dots on panel B and F indicate all known presence points collected from GBIF. The occurrences of GBIFs are distributed in with higher population fitness habitat $\text{Pr}(\lambda > 1)$, confirming that our study approach can reasonably predict range shifts.

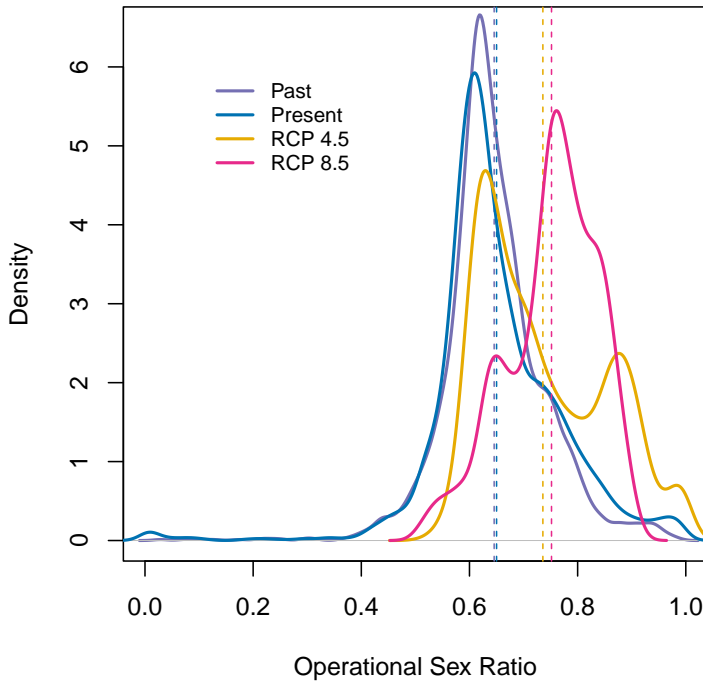


Figure 5: Change in Operational Sex Ratio (proportion of female panicle) over time (past, present, future). Future projections were based on the CMCC-CM model. The mean sex ratio for each time period is shown as vertical dashed line.

380 Discussion

381 Dioecious species make up a large fraction of Earth's biodiversity – most animals and many
 382 plants – yet we have little knowledge about how sex-specific demography and responses to
 383 climate drivers may affect population viability and range shifts of dioecious species under
 384 climate change. We used demographic data collected from common garden experiments,
 385 hierarchical Bayesian statistical modeling, and sex-structured demographic modeling to
 386 forecast for the first time the likely impact of climate change on range dynamics of a dioecious
 387 species. We found that demographic rates of Texas bluegrass and their sensitivities to climate
 388 drivers show significant sex bias, with females out-performing males, on average, and high
 389 and low temperature extremes disproportionately favoring female reproduction, leading to
 390 female skew in the operational sex ratio. In fact, we show that future climate change will likely
 391 not only shift this species' geographic niche northward, but it will also skew operational sex
 392 ratios toward stronger female bias. Our two-sex modeling framework accounts for reductions
 393 in female fertility with increasing female bias, and therefore predicts a narrower climatic niche

394 than the corresponding female-dominant model that ignores the feedback between population
395 structure and vital rates. Failure to account for population sex structure can therefore lead to
396 overestimation of suitable niche space and underestimation of range shifts under global change.

397 Our finding that climate change in the south-central US will likely lead to female-biased
398 operational sex ratios contrasts with previous studies of dioecious plants. While a baseline
399 female demographic advantage has been observed in several dioecious species (Bawa, 1980;
400 Sasaki et al., 2019; Zhao et al., 2012), focused on sex-specific sensitivity to climate drivers
401 predict an increase in male frequency in response to climate change (Hultine et al., 2016; Petry
402 et al., 2016). We speculate that differences in the costs of reproduction related to pollination
403 mode may help explain which sex is favored under climate stress. For most dioecious plant
404 species, the cost of reproduction is often higher for females than males due to the requirement
405 to develop seeds and fruits (Hultine et al., 2016). However, several studies reported a higher
406 cost of reproduction for males in wind pollinated species due to the larger amounts of pollen
407 they produce (Bruijning et al., 2017; Bürli et al., 2022; Cipollini and Whigham, 1994; Field
408 et al., 2013). Additional comparative studies across species that differ in life history traits
409 are needed to draw inferences regarding which types of species are likely to become female-
410 or male-biased in response to global change stressors.

411 While a two-sex modeling approach clearly adds biological realism, it was also additional
412 work (in the form of experiments, data, equations, code, and computation). Was it worth the
413 trouble? Generally, we suggest the answer should depend on the aims of the investigator.
414 Predictions of the sex-structured and female-dominant models were in strong agreement about
415 climate niche optima, and LTRE decomposition suggested that female vital rates determine
416 population responses to climate variation much more so than male vital rates. If we wanted
417 to know whether a poleward range shift is likely for Texas bluegrass, the simpler female-
418 dominant approach could have given us the correct answer. But more focused questions,
419 especially around the edges of niche space where sex ratio skew is more likely to impair
420 population viability, may require an explicit accounting for sex structure. If we aimed to
421 identify specific regions that are more or less inclined toward contraction or expansion, or sites
422 that might be suitable for assisted migration, we might reach qualitatively different conclusions
423 with female-dominant and two-sex models. For example, the female-dominant model is over-
424 confident that large swaths of Oklahoma will remain marginally suitable for Texas bluegrass
425 under the business-as-usual emissions scenario, while the two-sex model is more pessimistic,
426 because this region will become too female-biased to support viable populations. More
427 generally, we hypothesize that accounting for sex structure should be most important under
428 conditions that are already near the limits of population viability, where effects of mate
429 limitation could be more consequential. This suggests a particularly important role of sex-

430 structured modeling for threatened and endangered species, as conservation biologists have
431 already recognized (Jenouvrier et al., 2012; Milner-Gulland, 1994; Molnár et al., 2010).

432 Our results suggest that climate change, and specifically climate warming, will
433 drive a classic pattern of poleward expansion: contraction at the southern trailing edge
434 due to temperatures exceeding tolerable limits and expansion at the northern leading
435 edge due to release from low temperature limitation. Our statistical models captured
436 temperature-dependence in a phenomenological way, and the physiological mechanisms
437 underlying these responses remain to be explored. Increasing temperature could increase
438 evaporative demand, affect plant phenology (Iler et al., 2019; McLean et al., 2016; Sherry et al.,
439 2007), and germination rate (Reed et al., 2021). The potential for temperature to influence
440 these different processes changes seasonally (Konapala et al., 2020). For example, studies
441 suggested that species that are active during the growing season such as cool grass species
442 can have delayed phenology in response to global warming, particularly if temperatures rise
443 above their physiological tolerances (Cleland et al., 2007; Williams et al., 2015).

444 Regardless of the mechanism, it is clear that climate warming will generate leading
445 and trailing edges. Whether and at what pace the realized species' distribution tracks
446 geographic changes in suitable niche space is a different, open question. Expansion of the
447 leading edge could lag behind availability of suitable habitat due to dispersal limitation
448 (Pagel et al., 2020), and legacies of long-lived individuals can promote persistence of trailing
449 edge populations even as environmental conditions deteriorate (Margaret EK et al., 2023).
450 Environmentally-explicit demographic models are emerging as powerful tools to understand
451 and predicts the limits of population viability under global change (Merow et al., 2017;
452 Schultz et al., 2022), but incorporating non-equilibrium dynamics that emerge from dispersal
453 limitation and and historical legacies is an important new direction for this field.

454 Our forecasts for responses to climate change in Texas bluegrass should be interpreted
455 in light of several features of our study design. First, the design of our common garden
456 experiment and statistical modeling means that our geographic projections correspond
457 to an "average" genotype from across the range of Texas bluegrass. Local adaptation to
458 climate could make southern and northern edge populations more resilient to high and low
459 temperature stress, respectively, than the range-wide average (Angert et al., 2020; Gilbert
460 et al., 2017). The role of local adaptation in mitigating population response to climate is
461 an important next step in forecasting species' responses to global change . Second, as is
462 true for many ecological systems, future climate is likely to include conditions that have
463 no present-day analog (Intergovernmental Panel On Climate Change (Ipcc), 2023), a major
464 challenge for ecological forecasting. The years and locations of our experiment provided
465 us with unusually good coverage of likely past, present, and future conditions expected

466 throughout the study region, but we still had to extrapolate the statistical models to predict
467 responses to colder winter temperatures (that were more common in the past) and hotter
468 summer temperatures (that are expected in the future) than we directly observed (Fig. 1).
469 By employing a probabilistic measure of niche and geographic suitability ($Pr(\lambda) \geq 1$), our
470 projections account for the uncertainty associated with these extrapolated climate responses,
471 but there would be value in combining the spatiotemporal sampling of a common garden
472 design with experimental manipulations that push systems toward historical and/or future
473 conditions. Third, while we incorporated uncertainty associated with parameter estimation
474 and process error, there is additional uncertainty in future climate conditions. Future forecasts
475 for Texas bluegrass were generally consistent across different global circulation models
476 (reference supp figures), but combining uncertainty in future conditions alongside uncertainty
477 in biological responses to those conditions is an important frontier in ecological forecasting (?).

478 Conclusion

479 We investigated how demographic differences between the sexes and contrasting sensitivity to
480 climate can drive skewness in sex ratio on and possible range shifts in the context of climate
481 change. For Texas bluegrass, the future is female, and it is in Kansas. Our results suggest
482 that tracking only females could lead to an underestimation of the effect of climate change
483 on population dynamics, because it misses the feedback between population structure and
484 female fertility. But in broad strokes, a female-dominant perspective tells much of the story,
485 and that will likely be true for dioecious plants and animals with mating systems in which
486 few males can fertilize many females. Our work also provides a framework for predicting
487 the impact of global change on population dynamics and range shifts using probabilistic
488 measures that can incorporate and pick apart the many types of uncertainty that arise when
489 reconstructing the past or forecasting the future.

490 Acknowledgements

491 This research was supported by National Science Foundation Division of Environmental
492 Biology awards 2208857 and 2225027. We thank the organizations and institutions who hosted
493 us at their field station facilities, including The Nature Conservancy, Sam Houston State
494 University, University of Texas, Texas A&M University, Texas Tech University, Lake Lewisville
495 Environmental Learning Area, Wichita State University, and Pittsburgh State University.

496 **References**

- 497 Angert, A. L., Bontrager, M. G., and Ågren, J. (2020). What do we really know about adaptation
498 at range edges? *Annual Review of Ecology, Evolution, and Systematics*, 51(1):341–361.
- 499 Bawa, K. S. (1980). Evolution of dioecy in flowering plants. *Annual review of ecology and*
500 *systematics*, 11:15–39.
- 501 Bertrand, R., Lenoir, J., Piedallu, C., Riofrío-Dillon, G., De Ruffray, P., Vidal, C., Pierrat, J.-C.,
502 and Gégout, J.-C. (2011). Changes in plant community composition lag behind climate
503 warming in lowland forests. *Nature*, 479(7374):517–520.
- 504 Bruijning, M., Visser, M. D., Muller-Landau, H. C., Wright, S. J., Comita, L. S., Hubbell, S. P.,
505 de Kroon, H., and Jongejans, E. (2017). Surviving in a cosexual world: A cost-benefit
506 analysis of dioecy in tropical trees. *The American Naturalist*, 189(3):297–314.
- 507 Bürli, S., Pannell, J. R., and Tonnabel, J. (2022). Environmental variation in sex ratios and
508 sexual dimorphism in three wind-pollinated dioecious plant species. *Oikos*, 2022(6):e08651.
- 509 Caswell, H. (1989). Analysis of life table response experiments i. decomposition of effects
510 on population growth rate. *Ecological Modelling*, 46(3-4):221–237.
- 511 Caswell, H. (2000). *Matrix population models*, volume 1. Sinauer Sunderland, MA.
- 512 Cipollini, M. L. and Whigham, D. F. (1994). Sexual dimorphism and cost of reproduction
513 in the dioecious shrub *lindera benzoin* (lauraceae). *American Journal of Botany*, 81(1):65–75.
- 514 Cleland, E. E., Chuine, I., Menzel, A., Mooney, H. A., and Schwartz, M. D. (2007). Shifting
515 plant phenology in response to global change. *Trends in ecology & evolution*, 22(7):357–365.
- 516 Compagnoni, A., Steigman, K., and Miller, T. E. (2017). Can't live with them, can't live
517 without them? balancing mating and competition in two-sex populations. *Proceedings of*
518 *the Royal Society B: Biological Sciences*, 284(1865):20171999.
- 519 Czachura, K. and Miller, T. E. (2020). Demographic back-casting reveals that subtle
520 dimensions of climate change have strong effects on population viability. *Journal of Ecology*,
521 108(6):2557–2570.
- 522 Dahlgren, J. P., Bengtsson, K., and Ehrlén, J. (2016). The demography of climate-driven and
523 density-regulated population dynamics in a perennial plant. *Ecology*, 97(4):899–907.

- 524 Davis, M. B. and Shaw, R. G. (2001). Range shifts and adaptive responses to quaternary
525 climate change. *Science*, 292(5517):673–679.
- 526 Diez, J. M., Giladi, I., Warren, R., and Pulliam, H. R. (2014). Probabilistic and spatially variable
527 niches inferred from demography. *Journal of ecology*, 102(2):544–554.
- 528 Eberhart-Phillips, L. J., Küpper, C., Miller, T. E., Cruz-López, M., Maher, K. H., Dos Remedios,
529 N., Stoffel, M. A., Hoffman, J. I., Krüger, O., and Székely, T. (2017). Sex-specific early
530 survival drives adult sex ratio bias in snowy plovers and impacts mating system and
531 population growth. *Proceedings of the National Academy of Sciences*, 114(27):E5474–E5481.
- 532 Ehrlén, J. and Morris, W. F. (2015). Predicting changes in the distribution and abundance
533 of species under environmental change. *Ecology letters*, 18(3):303–314.
- 534 Elderd, B. D. and Miller, T. E. (2016). Quantifying demographic uncertainty: Bayesian methods
535 for integral projection models. *Ecological Monographs*, 86(1):125–144.
- 536 Ellis, R. P., Davison, W., Queirós, A. M., Kroeker, K. J., Calosi, P., Dupont, S., Spicer, J. I.,
537 Wilson, R. W., Widdicombe, S., and Urbina, M. A. (2017). Does sex really matter? explaining
538 intraspecies variation in ocean acidification responses. *Biology letters*, 13(2):20160761.
- 539 Ellner, S. P., Adler, P. B., Childs, D. Z., Hooker, G., Miller, T. E., and Rees, M. (2022). A critical
540 comparison of integral projection and matrix projection models for demographic analysis:
541 Comment. *Ecology*.
- 542 Ellner, S. P., Childs, D. Z., Rees, M., et al. (2016). Data-driven modelling of structured
543 populations. *A practical guide to the Integral Projection Model*. Cham: Springer.
- 544 Evans, M. E., Merow, C., Record, S., McMahon, S. M., and Enquist, B. J. (2016). Towards
545 process-based range modeling of many species. *Trends in Ecology & Evolution*, 31(11):860–871.
- 546 Field, D. L., Pickup, M., and Barrett, S. C. (2013). Comparative analyses of sex-ratio variation
547 in dioecious flowering plants. *Evolution*, 67(3):661–672.
- 548 Gamelon, M., Grøtan, V., Nilsson, A. L., Engen, S., Hurrell, J. W., Jerstad, K., Phillips, A. S.,
549 Røstad, O. W., Slagsvold, T., Walseng, B., et al. (2017). Interactions between demography
550 and environmental effects are important determinants of population dynamics. *Science
Advances*, 3(2):e1602298.
- 552 Gerber, L. R. and White, E. R. (2014). Two-sex matrix models in assessing population viability:
553 when do male dynamics matter? *Journal of Applied Ecology*, 51(1):270–278.

- 554 Gilbert, K. J., Sharp, N. P., Angert, A. L., Conte, G. L., Draghi, J. A., Guillaume, F., Hargreaves,
555 A. L., Matthey-Doret, R., and Whitlock, M. C. (2017). Local adaptation interacts with
556 expansion load during range expansion: maladaptation reduces expansion load. *The*
557 *American Naturalist*, 189(4):368–380.
- 558 Gissi, E., Bowyer, R. T., and Bleich, V. C. (2024). Sex-based differences affect conservation.
559 *Science*, 384(6702):1309–1310.
- 560 Gissi, E., Schiebinger, L., Hadly, E. A., Crowder, L. B., Santoleri, R., and Micheli, F. (2023).
561 Exploring climate-induced sex-based differences in aquatic and terrestrial ecosystems to
562 mitigate biodiversity loss. *nature communications*, 14(1):4787.
- 563 Hernández, C. M., Ellner, S. P., Adler, P. B., Hooker, G., and Snyder, R. E. (2023). An exact
564 version of life table response experiment analysis, and the r package exactltre. *Methods*
565 in *Ecology and Evolution*, 14(3):939–951.
- 566 Hitchcock, A. S. (1971). *Manual of the grasses of the United States*, volume 2. Courier Corporation.
- 567 Hultine, K. R., Grady, K. C., Wood, T. E., Shuster, S. M., Stella, J. C., and Whitham, T. G. (2016).
568 Climate change perils for dioecious plant species. *Nature Plants*, 2(8):1–8.
- 569 Iler, A. M., Compagnoni, A., Inouye, D. W., Williams, J. L., CaraDonna, P. J., Anderson, A., and
570 Miller, T. E. (2019). Reproductive losses due to climate change-induced earlier flowering are
571 not the primary threat to plant population viability in a perennial herb. *Journal of Ecology*,
572 107(4):1931–1943.
- 573 Intergovernmental Panel On Climate Change (Ipcc) (2023). *Climate Change 2022 – Impacts,
574 Adaptation and Vulnerability: Working Group II Contribution to the Sixth Assessment Report of
575 the Intergovernmental Panel on Climate Change*. Cambridge University Press, 1 edition.
- 576 Jenouvrier, S., Holland, M., Stroeve, J., Barbraud, C., Weimerskirch, H., Serreze, M., and
577 Caswell, H. (2012). Effects of climate change on an emperor penguin population: analysis
578 of coupled demographic and climate models. *Global Change Biology*, 18(9):2756–2770.
- 579 Jones, M. H., Macdonald, S. E., and Henry, G. H. (1999). Sex-and habitat-specific responses
580 of a high arctic willow, salix arctica, to experimental climate change. *Oikos*, pages 129–138.
- 581 Karger, D. N., Conrad, O., Böhner, J., Kawohl, T., Kreft, H., Soria-Auza, R. W., Zimmermann,
582 N. E., Linder, H. P., and Kessler, M. (2017). Climatologies at high resolution for the earth’s
583 land surface areas. *Scientific data*, 4(1):1–20.

- 584 Kindiger, B. (2004). Interspecific hybrids of *poa arachnifera* × *poa secunda*. *Journal of New*
585 *Seeds*, 6(1):1–26.
- 586 Konapala, G., Mishra, A. K., Wada, Y., and Mann, M. E. (2020). Climate change will affect
587 global water availability through compounding changes in seasonal precipitation and
588 evaporation. *Nature communications*, 11(1):3044.
- 589 Lee-Yaw, J. A., Kharouba, H. M., Bontrager, M., Mahony, C., Csergő, A. M., Noreen, A. M.,
590 Li, Q., Schuster, R., and Angert, A. L. (2016). A synthesis of transplant experiments and
591 ecological niche models suggests that range limits are often niche limits. *Ecology letters*,
592 19(6):710–722.
- 593 Liaw, A., Wiener, M., et al. (2002). Classification and regression by randomforest. *R news*,
594 2(3):18–22.
- 595 Louthan, A. M., Keighron, M., Kiekebusch, E., Cayton, H., Terando, A., and Morris, W. F.
596 (2022). Climate change weakens the impact of disturbance interval on the growth rate of
597 natural populations of venus flytrap. *Ecological Monographs*, 92(4):e1528.
- 598 Lynch, H. J., Rhainds, M., Calabrese, J. M., Cantrell, S., Cosner, C., and Fagan, W. F. (2014).
599 How climate extremes—not means—define a species' geographic range boundary via a
600 demographic tipping point. *Ecological Monographs*, 84(1):131–149.
- 601 Margaret EK, E., Sharmila MN, D., Heilman, K. A., Tipton, J. R., DeRose, R. J., Stefan, K.,
602 Schultz, E. L., and Shaw, J. D. (2023). The trailing edge is everywhere: tree rings reveal
603 the transient risk of extinction hidden inside climate envelope forecasts. Technical report,
604 Los Alamos National Laboratory (LANL), Los Alamos, NM (United States).
- 605 McLean, N., Lawson, C. R., Leech, D. I., and van de Pol, M. (2016). Predicting when climate-
606 driven phenotypic change affects population dynamics. *Ecology Letters*, 19(6):595–608.
- 607 Merow, C., Bois, S. T., Allen, J. M., Xie, Y., and Silander Jr, J. A. (2017). Climate change both
608 facilitates and inhibits invasive plant ranges in new england. *Proceedings of the National*
609 *Academy of Sciences*, 114(16):E3276–E3284.
- 610 Miller, T. and Compagnoni, A. (2022a). Data from: Two-sex demography, sexual niche
611 differentiation, and the geographic range limits of texas bluegrass (*Poa arachnifera*). *American*
612 *Naturalist*, Dryad Digital Repository,. <https://doi.org/10.5061/dryad.kkwh70s5x>.

- 613 Miller, T. E. and Compagnoni, A. (2022b). Two-sex demography, sexual niche differentiation,
614 and the geographic range limits of Texas bluegrass (*Poa arachnifera*). *The American
615 Naturalist*, 200(1):17–31.
- 616 Miller, T. E., Shaw, A. K., Inouye, B. D., and Neubert, M. G. (2011). Sex-biased dispersal and
617 the speed of two-sex invasions. *The American Naturalist*, 177(5):549–561.
- 618 Milner-Gulland, E. (1994). A population model for the management of the saiga antelope.
619 *Journal of Applied Ecology*, pages 25–39.
- 620 Molnár, P. K., Derocher, A. E., Thiemann, G. W., and Lewis, M. A. (2010). Predicting survival,
621 reproduction and abundance of polar bears under climate change. *Biological Conservation*,
622 143(7):1612–1622.
- 623 Morrison, C. A., Robinson, R. A., Clark, J. A., and Gill, J. A. (2016). Causes and consequences
624 of spatial variation in sex ratios in a declining bird species. *Journal of Animal Ecology*,
625 85(5):1298–1306.
- 626 Pagel, J., Treurnicht, M., Bond, W. J., Kraaij, T., Nottebrock, H., Schutte-Vlok, A., Tonnabel,
627 J., Esler, K. J., and Schurr, F. M. (2020). Mismatches between demographic niches and
628 geographic distributions are strongest in poorly dispersed and highly persistent plant
629 species. *Proceedings of the National Academy of Sciences*, 117(7):3663–3669.
- 630 Pease, C. M., Lande, R., and Bull, J. (1989). A model of population growth, dispersal and
631 evolution in a changing environment. *Ecology*, 70(6):1657–1664.
- 632 Petry, W. K., Soule, J. D., Iler, A. M., Chicas-Mosier, A., Inouye, D. W., Miller, T. E., and
633 Mooney, K. A. (2016). Sex-specific responses to climate change in plants alter population
634 sex ratio and performance. *Science*, 353(6294):69–71.
- 635 Piironen, J. and Vehtari, A. (2017). Comparison of bayesian predictive methods for model
636 selection. *Statistics and Computing*, 27:711–735.
- 637 Pottier, P., Burke, S., Drobniak, S. M., Lagisz, M., and Nakagawa, S. (2021). Sexual (in) equality?
638 a meta-analysis of sex differences in thermal acclimation capacity across ectotherms.
639 *Functional Ecology*, 35(12):2663–2678.
- 640 R Core Team (2023). *R: A Language and Environment for Statistical Computing*. R Foundation
641 for Statistical Computing, Vienna, Austria.

- 642 Reed, P. B., Peterson, M. L., Pfeifer-Meister, L. E., Morris, W. F., Doak, D. F., Roy, B. A., Johnson,
643 B. R., Bailes, G. T., Nelson, A. A., and Bridgham, S. D. (2021). Climate manipulations
644 differentially affect plant population dynamics within versus beyond northern range limits.
645 *Journal of Ecology*, 109(2):664–675.
- 646 Renganayaki, K., Jessup, R., Burson, B., Hussey, M., and Read, J. (2005). Identification of
647 male-specific aflp markers in dioecious texas bluegrass. *Crop science*, 45(6):2529–2539.
- 648 Sanderson, B. M., Knutti, R., and Caldwell, P. (2015). A representative democracy to reduce
649 interdependency in a multimodel ensemble. *Journal of Climate*, 28(13):5171–5194.
- 650 Sasaki, M., Hedberg, S., Richardson, K., and Dam, H. G. (2019). Complex interactions
651 between local adaptation, phenotypic plasticity and sex affect vulnerability to warming
652 in a widespread marine copepod. *Royal Society open science*, 6(3):182115.
- 653 Schultz, E. L., Hülsmann, L., Pillet, M. D., Hartig, F., Breshears, D. D., Record, S., Shaw, J. D.,
654 DeRose, R. J., Zuidema, P. A., and Evans, M. E. (2022). Climate-driven, but dynamic and
655 complex? a reconciliation of competing hypotheses for species' distributions. *Ecology letters*,
656 25(1):38–51.
- 657 Schwalm, C. R., Glendon, S., and Duffy, P. B. (2020). Rcp8. 5 tracks cumulative co2 emissions.
658 *Proceedings of the National Academy of Sciences*, 117(33):19656–19657.
- 659 Schwinning, S., Lortie, C. J., Esque, T. C., and DeFalco, L. A. (2022). What common-garden
660 experiments tell us about climate responses in plants.
- 661 Sexton, J. P., McIntyre, P. J., Angert, A. L., and Rice, K. J. (2009). Evolution and ecology of
662 species range limits. *Annu. Rev. Ecol. Evol. Syst.*, 40:415–436.
- 663 Shelton, A. O. (2010). The ecological and evolutionary drivers of female-biased sex ratios:
664 two-sex models of perennial seagrasses. *The American Naturalist*, 175(3):302–315.
- 665 Sherry, R. A., Zhou, X., Gu, S., Arnone III, J. A., Schimel, D. S., Verburg, P. S., Wallace,
666 L. L., and Luo, Y. (2007). Divergence of reproductive phenology under climate warming.
667 *Proceedings of the National Academy of Sciences*, 104(1):198–202.
- 668 Smith, M. D., Wilkins, K. D., Holdrege, M. C., Wilfahrt, P., Collins, S. L., Knapp, A. K., Sala,
669 O. E., Dukes, J. S., Phillips, R. P., Yahdjian, L., et al. (2024). Extreme drought impacts have
670 been underestimated in grasslands and shrublands globally. *Proceedings of the National
671 Academy of Sciences*, 121(4):e2309881120.

- 672 Stan Development Team (2023). RStan: the R interface to Stan. R package version 2.21.8.
- 673 Thomson, A. M., Calvin, K. V., Smith, S. J., Kyle, G. P., Volke, A., Patel, P., Delgado-Arias,
674 S., Bond-Lamberty, B., Wise, M. A., Clarke, L. E., et al. (2011). Rcp4. 5: a pathway for
675 stabilization of radiative forcing by 2100. *Climatic change*, 109:77–94.
- 676 Tognetti, R. (2012). Adaptation to climate change of dioecious plants: does gender balance
677 matter? *Tree Physiology*, 32(11):1321–1324.
- 678 Williams, J. L., Jacquemyn, H., Ochocki, B. M., Brys, R., and Miller, T. E. (2015). Life
679 history evolution under climate change and its influence on the population dynamics of
680 a long-lived plant. *Journal of Ecology*, 103(4):798–808.
- 681 Zhao, H., Li, Y., Zhang, X., Korpelainen, H., and Li, C. (2012). Sex-related and stage-dependent
682 source-to-sink transition in populus cathayana grown at elevated co 2 and elevated
683 temperature. *Tree Physiology*, 32(11):1325–1338.

Supporting Information

684 S.1 Supporting Figures

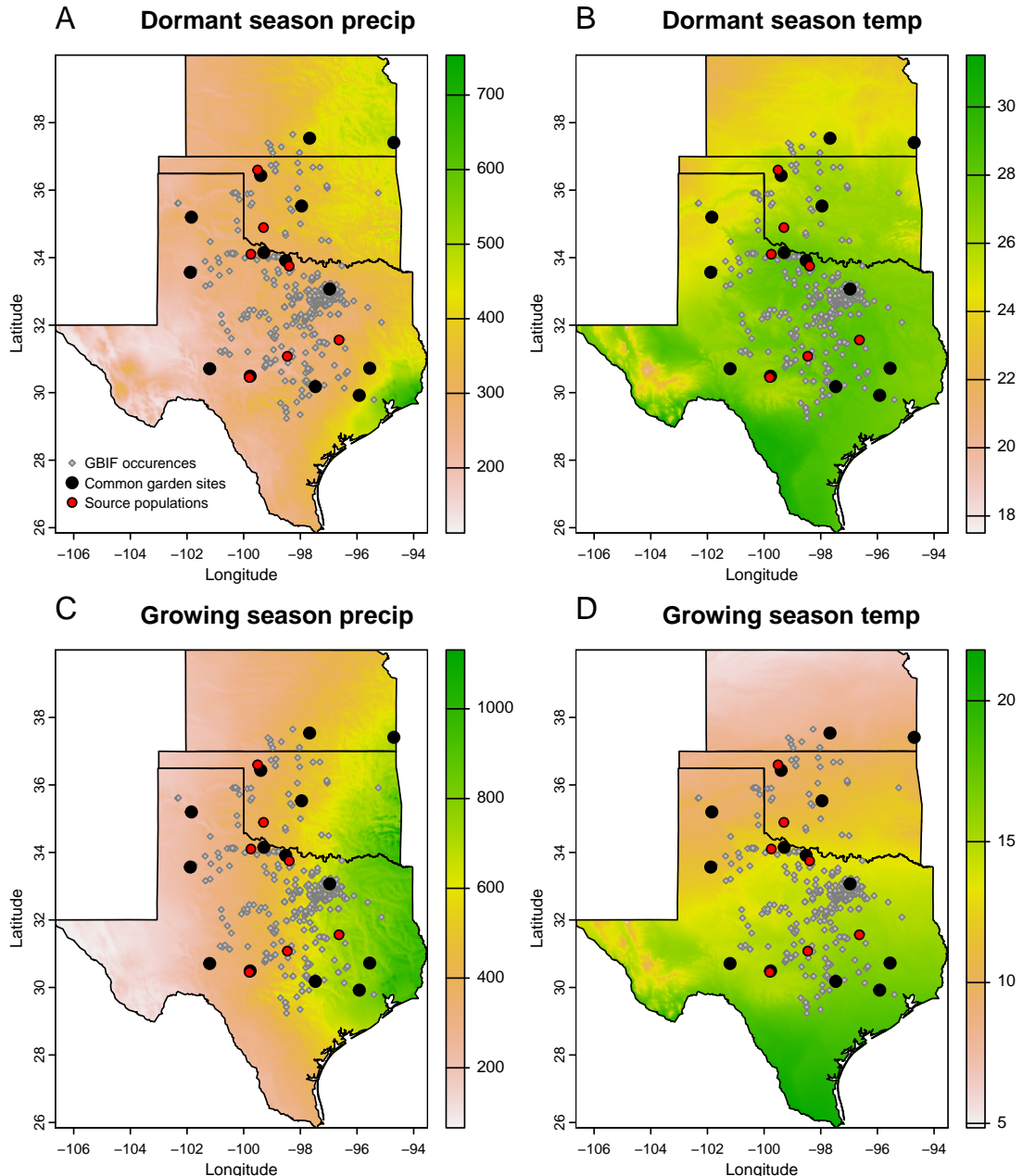


Figure S-1: Maps of 30-year (1990-2019) climate normals and study sites used for demographic monitoring of *Poa arachnifera* in Texas, Kansas and Oklahoma in the United States. Precipitation is in mm and temperature is in °C. We surveyed 22 natural populations (grey diamond). The common garden sites were installed on 14 sites (black circle) collected from 7 sources populations (red circle).

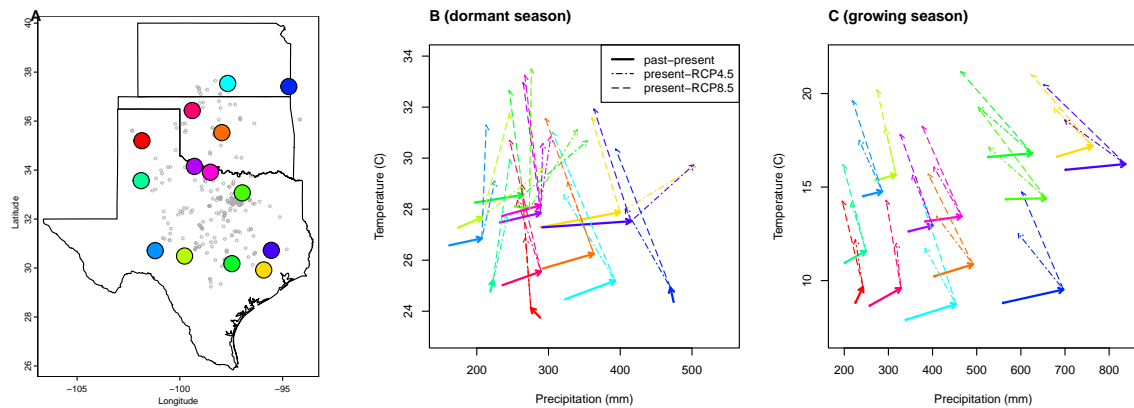


Figure S-2: (A), Common garden locations in Texas, Oklahoma, and Kansas (points) and (B,C) corresponding changes in growing and dormant season climate. Arrows in B,C connect past (1901-1930) and present (1990-2019) climate normals, and present and future (2071-2100) climate normals under RCP4.5 and RCP8.5 forecasts. Future forecasts are from MIROC5 but other climate models show similar patterns.

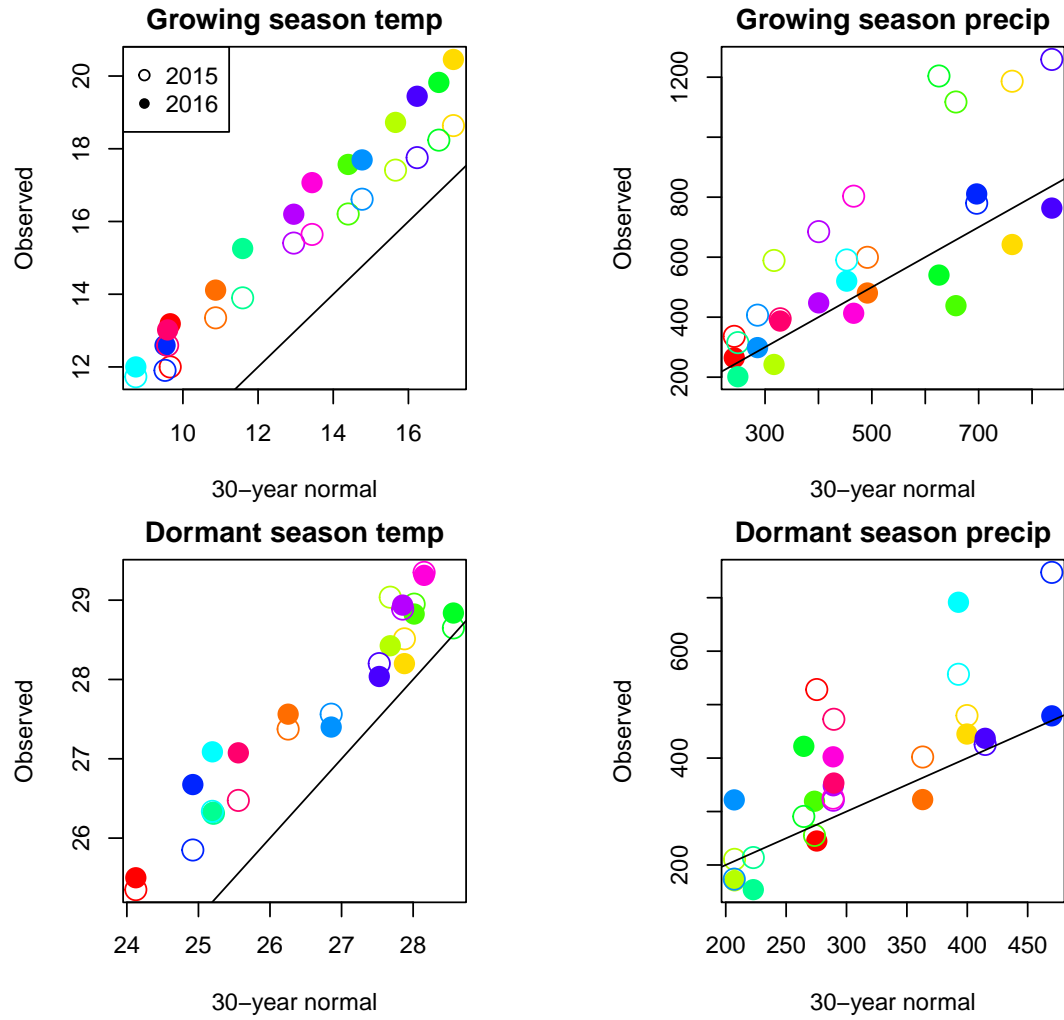


Figure S-3: Comparison of 30-year (1990-2019) climate normals and observed weather conditions at common garden sites during the 2014–15 and 2015–16 census periods. Temperature is in $^{\circ}\text{C}$ and precipitation is in mm . Colors represent sites and lines show the $y=x$ relationship.

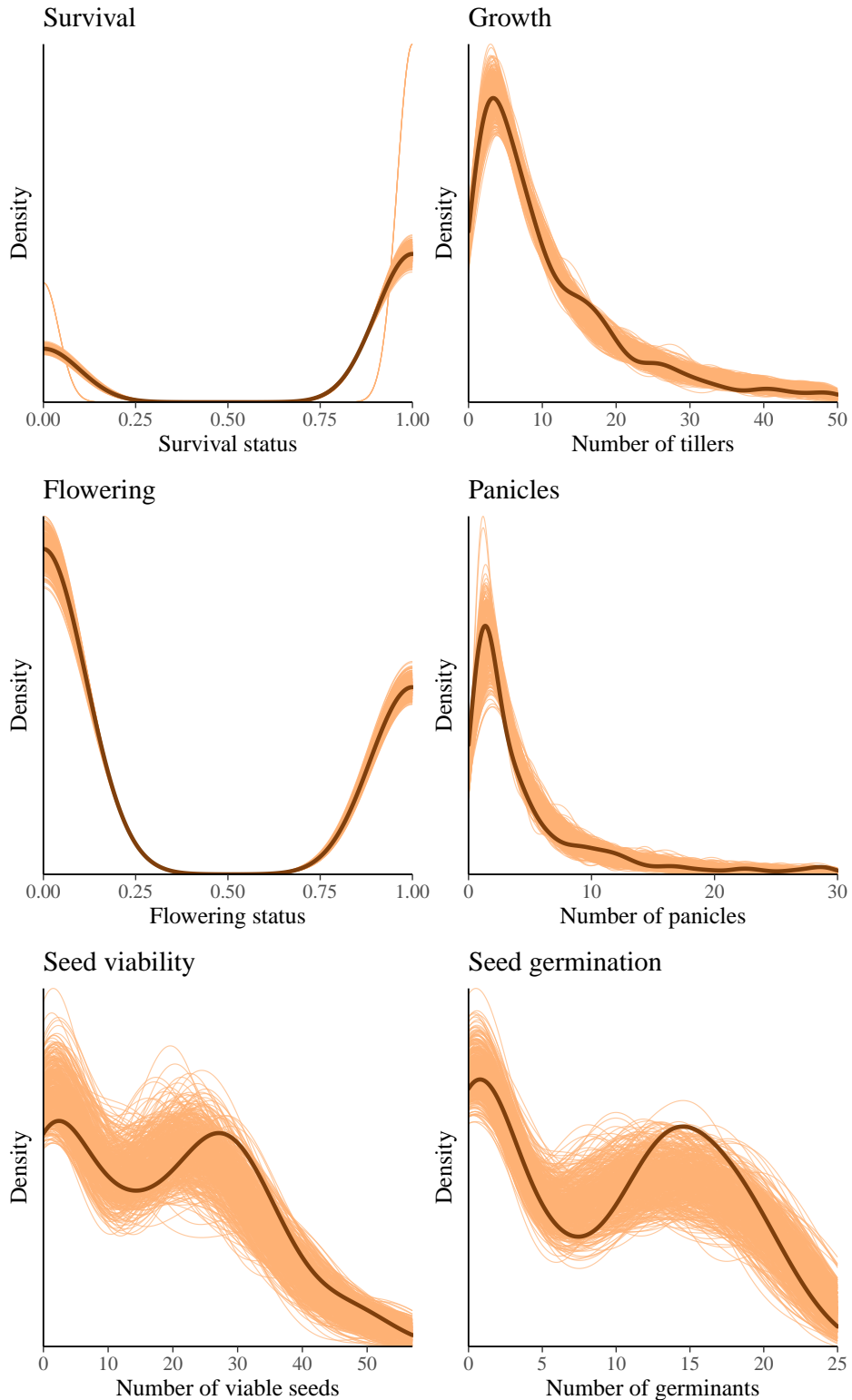


Figure S-4: Posterior predictive checks. Consistency between real data and simulated values suggests that the fitted vital rate models accurately describes the data. Graph shows density curves for the observed data (light orange) along with the simulated values (dark orange).

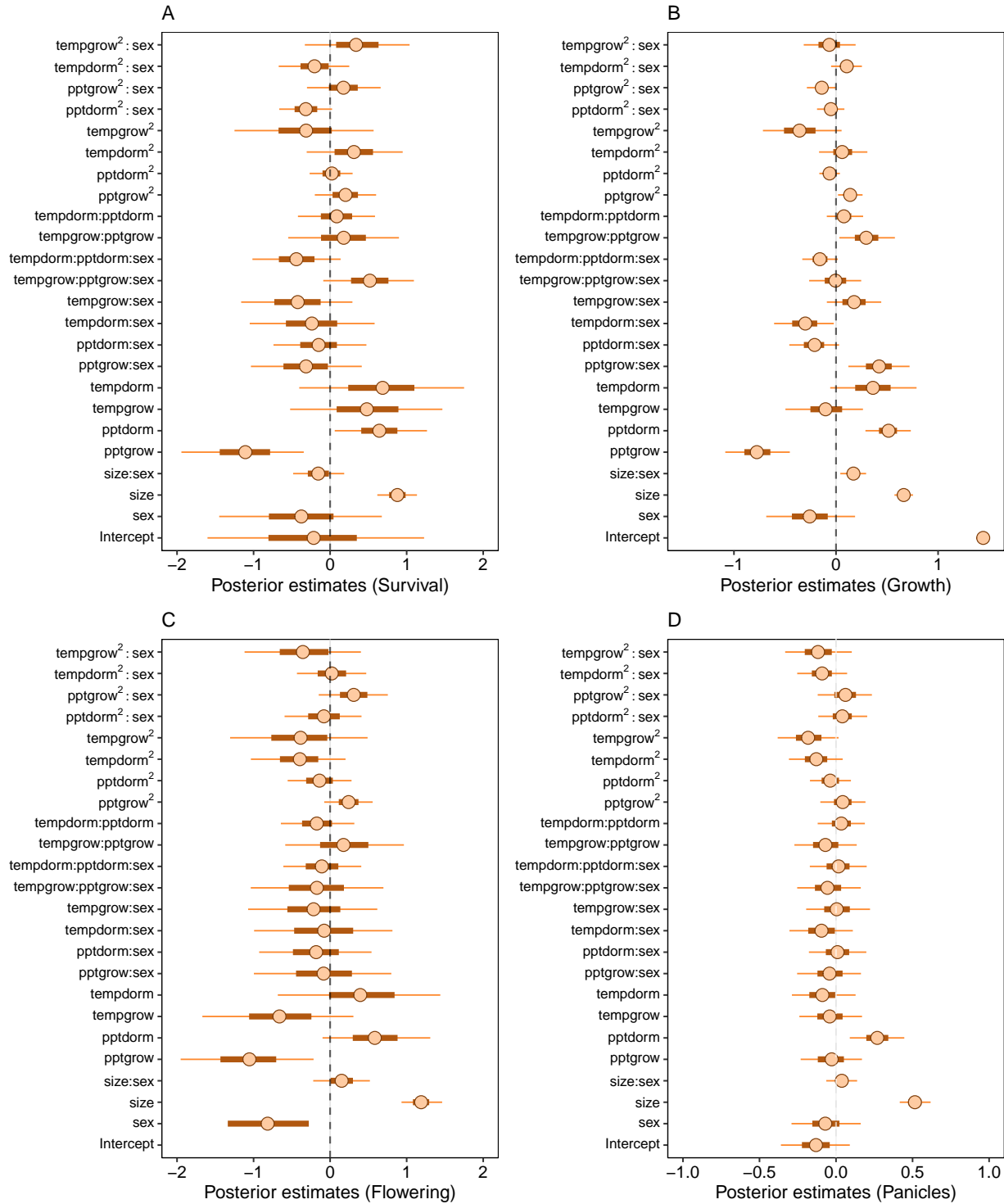


Figure S-5: Mean parameter values and 95% credible intervals of the posterior probability distributions. pptgrow is the precipitation of growing season, Tempgrow is the temperature of growing season, pptdorm is the temperature of dormant season, Tempdorm is the temperature of dormant season.

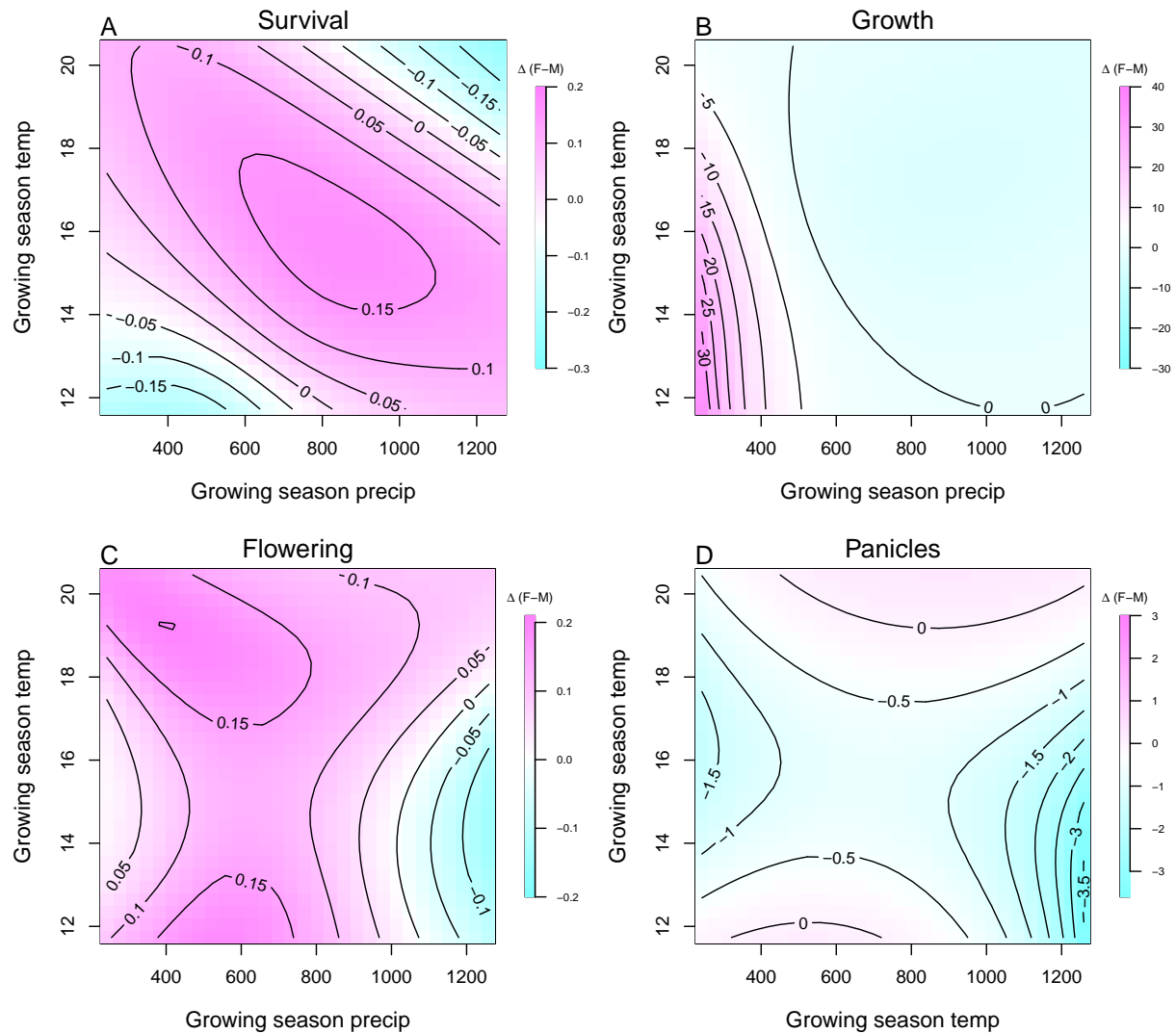


Figure S-6: Predicted difference in demographic response to climate across species range between female and male. Contours show predicted value of that difference conditional on precipitation and temperature of growing season

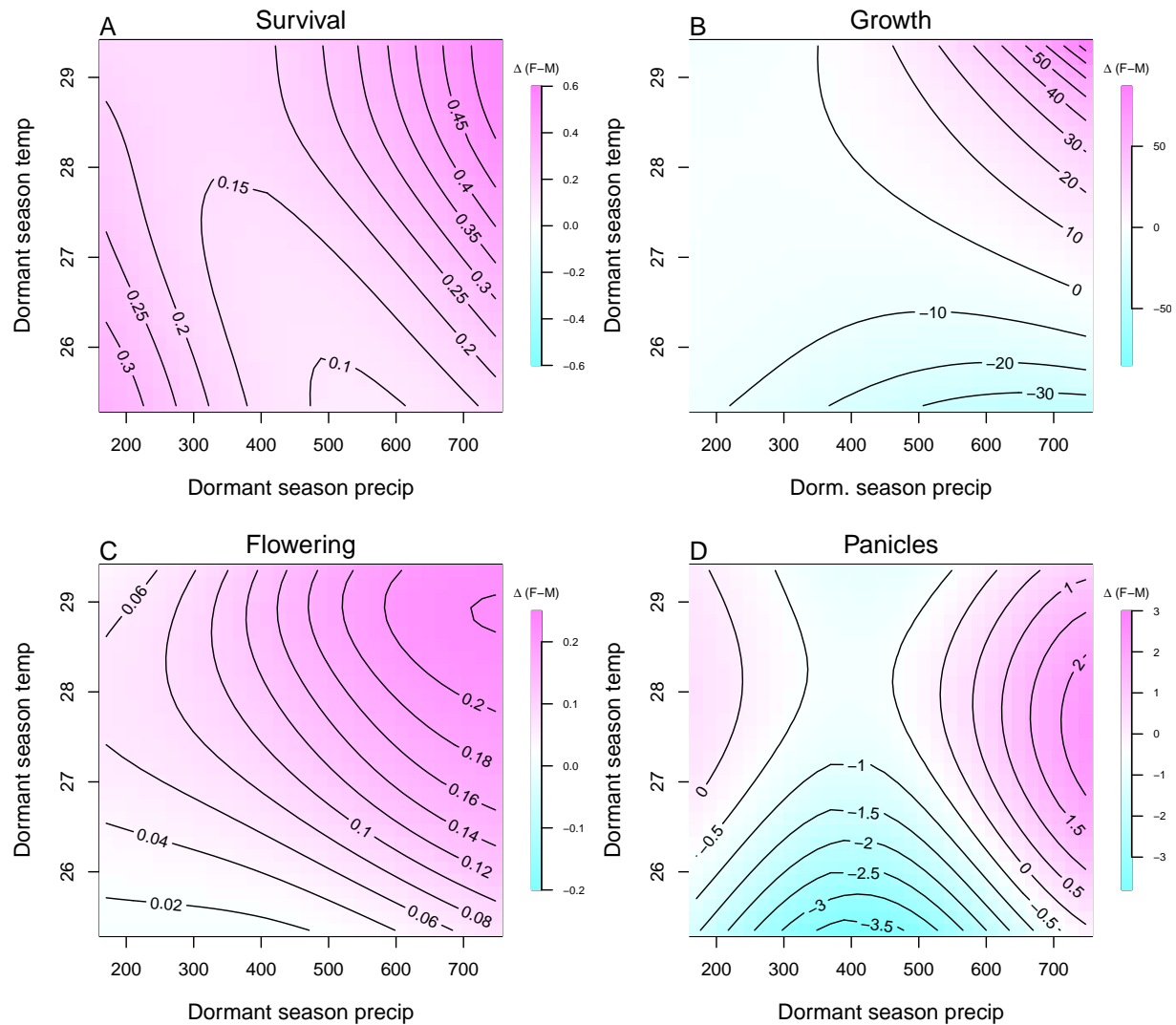


Figure S-7: Predicted difference in demographic response to climate across species range between female and male. Contours show predicted value of that difference conditional on precipitation and temperature of the dormant season

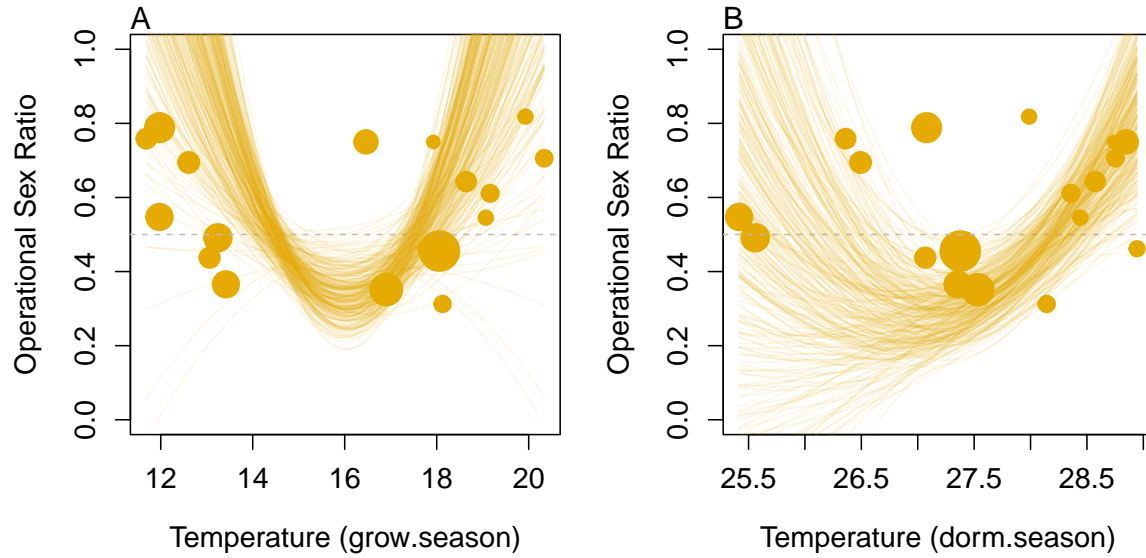


Figure S-8: Significant Operational Sex Ratio response across climate gradient. (A, B) Proportion of panicles that were females across temperature of the growing and dormant season

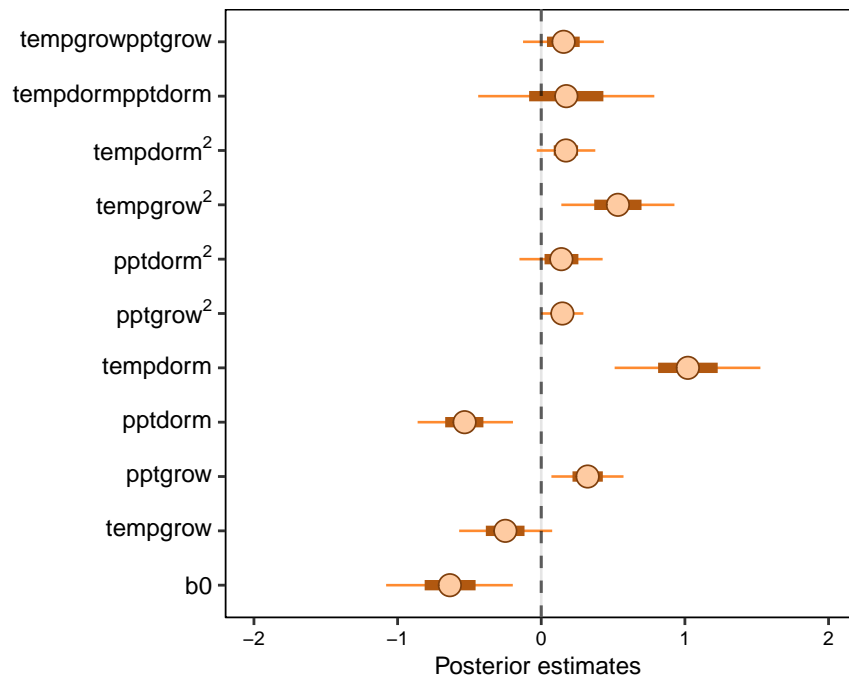


Figure S-9: Mean parameter values and 95% credible intervals of the posterior probability distributions for climate drivers of operational sex ratio (female fraction of total panicles) across common garden years and sites. pptgrow is the precipitation of growing season, Tempgrow is the temperature of growing season, pptdorm is the temperature of dormant season, Tempdorm is the temperature of dormant season.

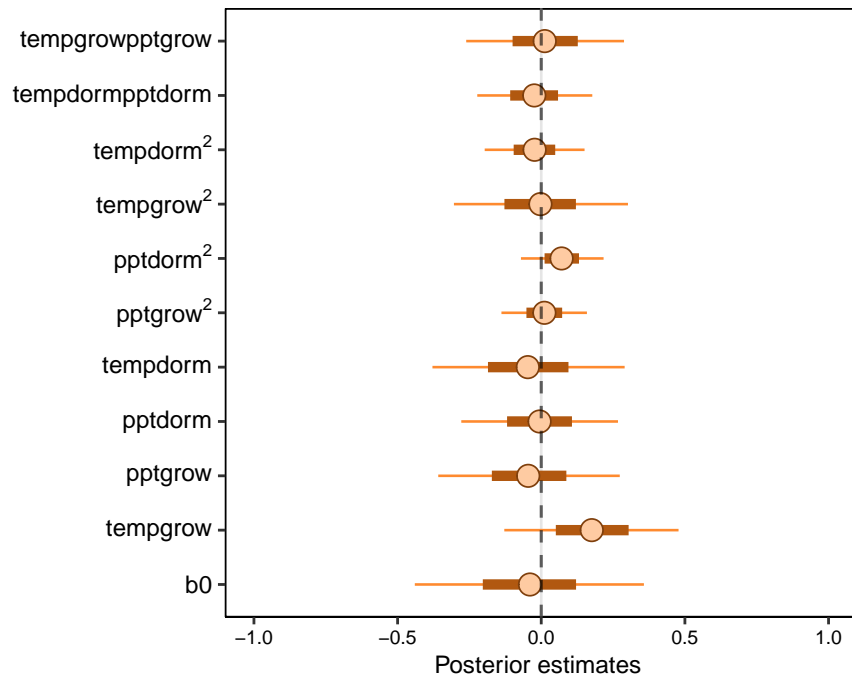


Figure S-10: Mean parameter values and 95% credible intervals of the posterior probability distributions for climate drivers of sex ratio (female fraction of the populations) across common garden years and sites. pptgrow is the precipitation of growing season, Tempgrow is the temperature of growing season, pptdorm is the temperature of dormant season, Tempdorm is the temperature of dormancy.

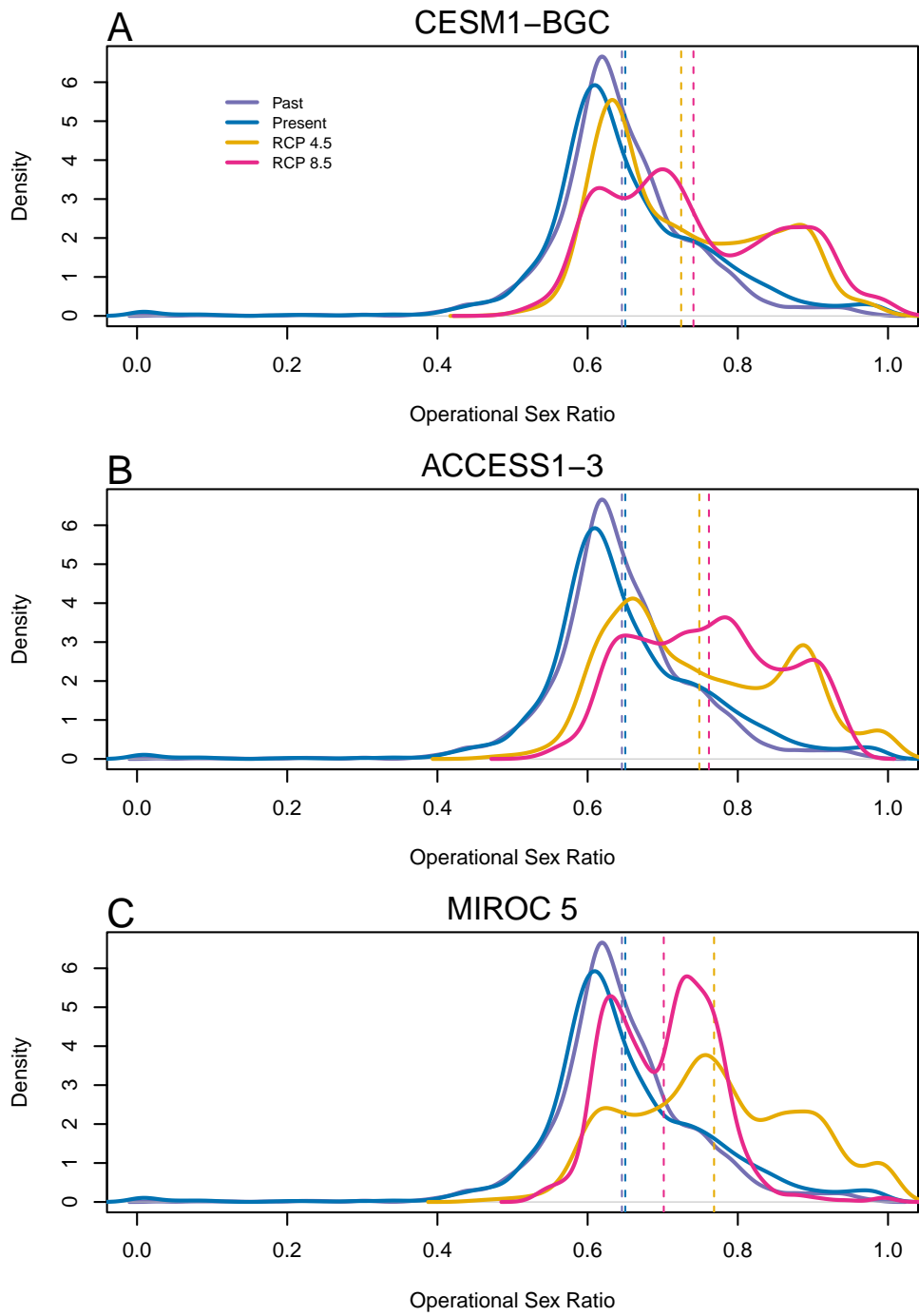


Figure S-11: Change in Operational Sex Ratio (proportion of female) over time (past, present, future). Future projections were based on A) MIROC 5, B) CES, C) ACC. The means for each model are shown as vertical dashed lines.

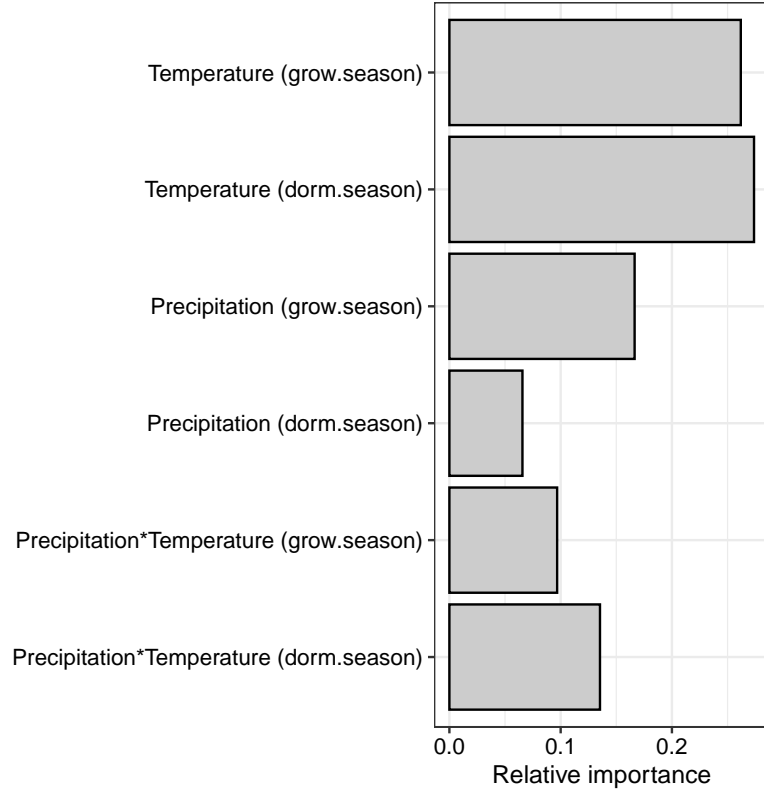


Figure S-12: Life Table Response Experiment: The bar represent the relative importance of each predictors.

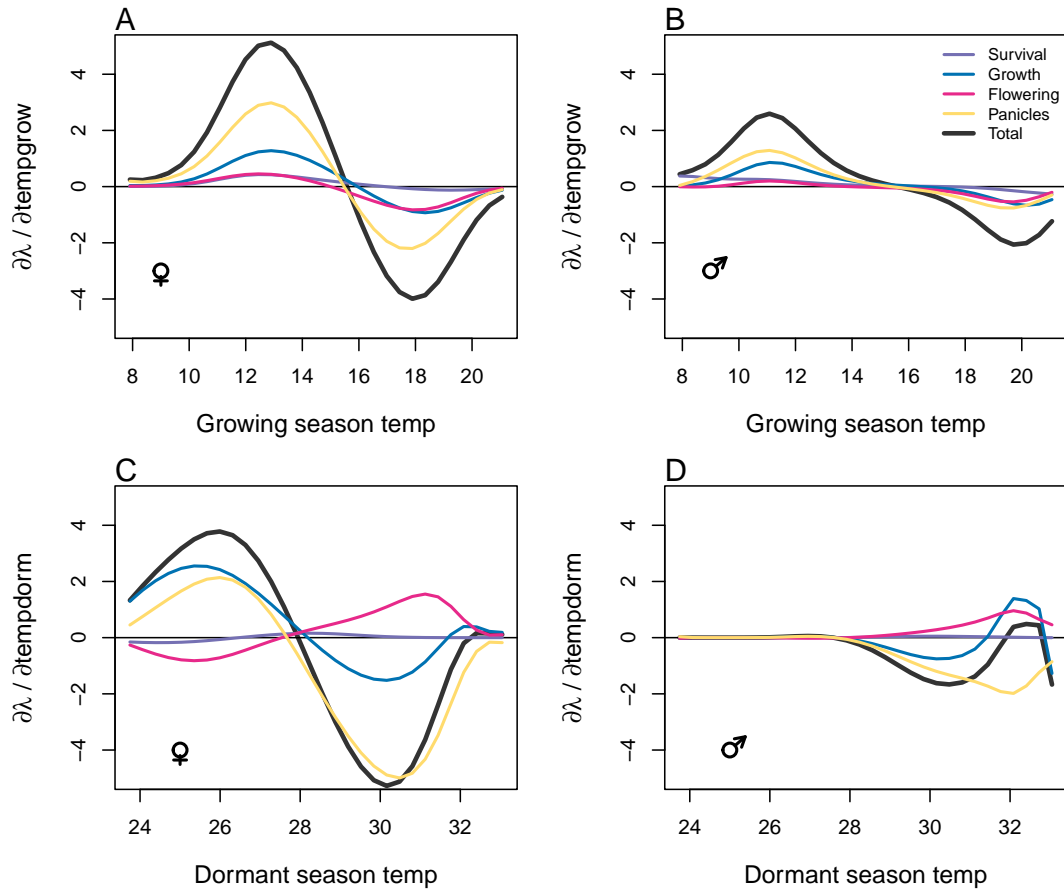


Figure S-13: Life table response experiment decomposition of the sensitivity of λ to seasonal climate into additive vital rate contributions of males and females based on posterior mean parameter estimates. (A) Temperature of growing season (contribution of female), (B) Temperature of growing season (contribution of male), (C) Temperature of dormant season (contribution of female) and (D) Temperature of dormant season (contribution of male).

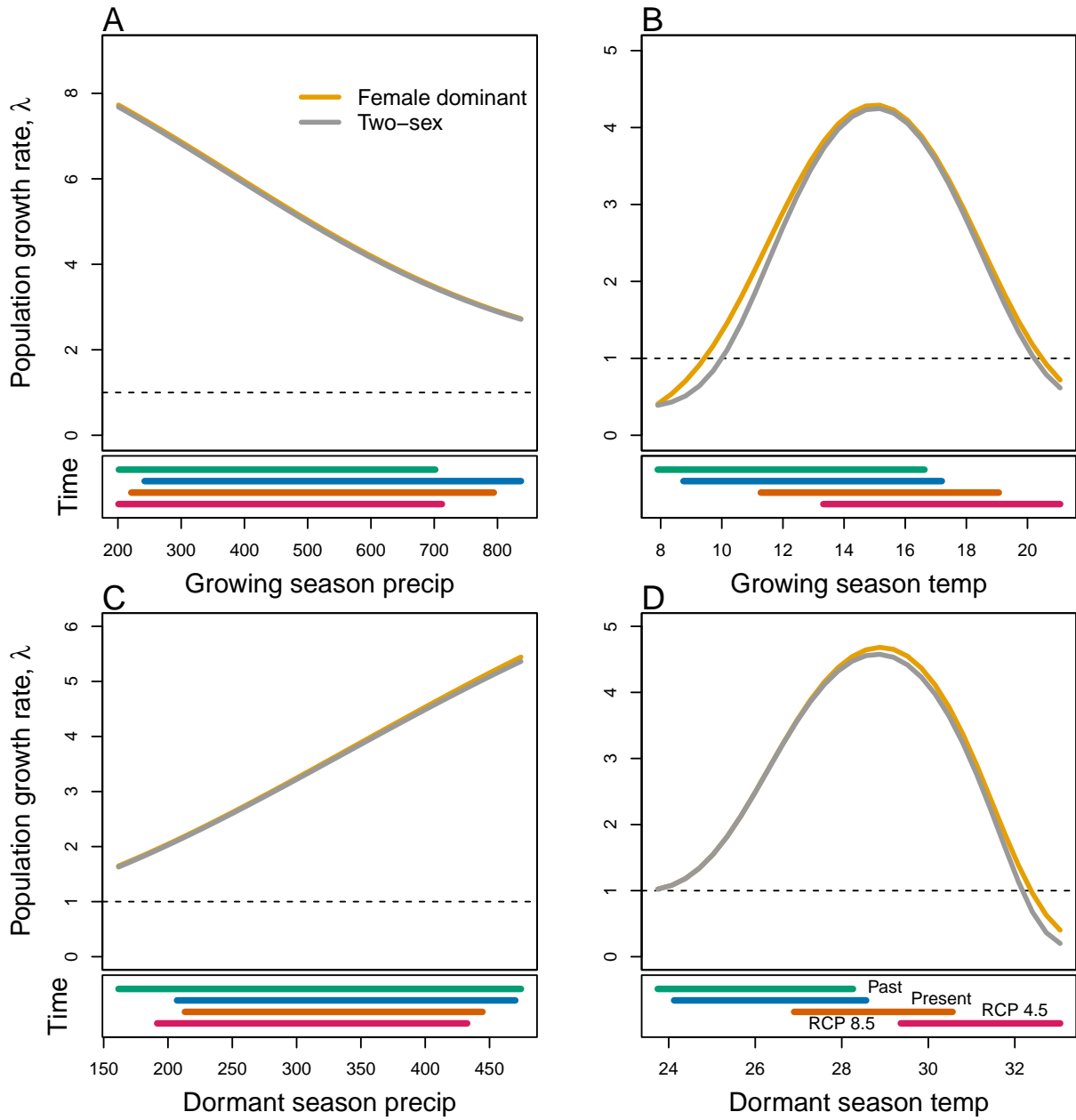


Figure S-14: Predicted population growth rate (λ) in different ranges of climate. (A) Precipitation of the growing season, (B) Temperature of the growing season, (C) Precipitation of the dormant season, (D) Temperature of the dormant season. The grey curve shows prediction by the two-sex matrix projection model that incorporates sex-specific demographic responses to climate with sex ratio dependent seed fertilization. The orange curve represents the prediction by the female dominant matrix projection model. The dashed horizontal line indicates the limit of population viability ($\lambda = 1$). Lower panels below each data panel show ranges of climate values for different time period (past climate, present and future climates). For future climate, we show a Representation Concentration Pathways (RCP) 4.5 and 8.5. Values population viability of (λ) are derived from the mean climate variables across 4 GCMs (MIROC5, ACCESS1-3, CESM1-BGC, CMCC-CM).

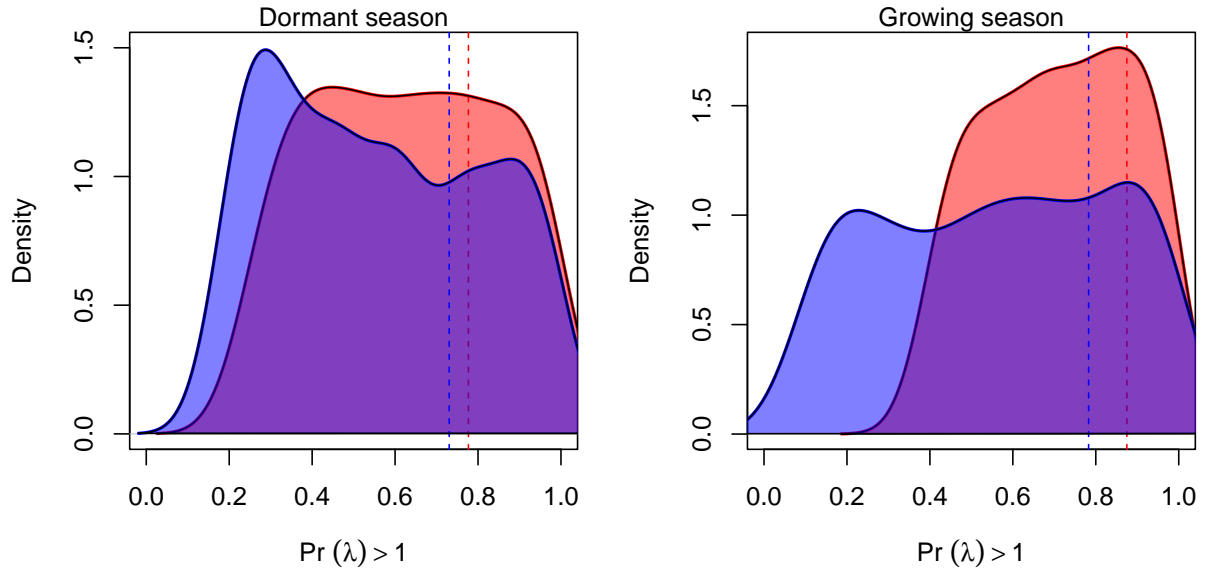


Figure S-15: Assessment of the statistical difference between the two-sex models and the female dominant model for the dormant and growing season. Plots show the density of $\Pr(\lambda > 1)$ values for female dominant (pink) and two-sex models (violet) for each season. The means for each model are shown as vertical dashed lines.

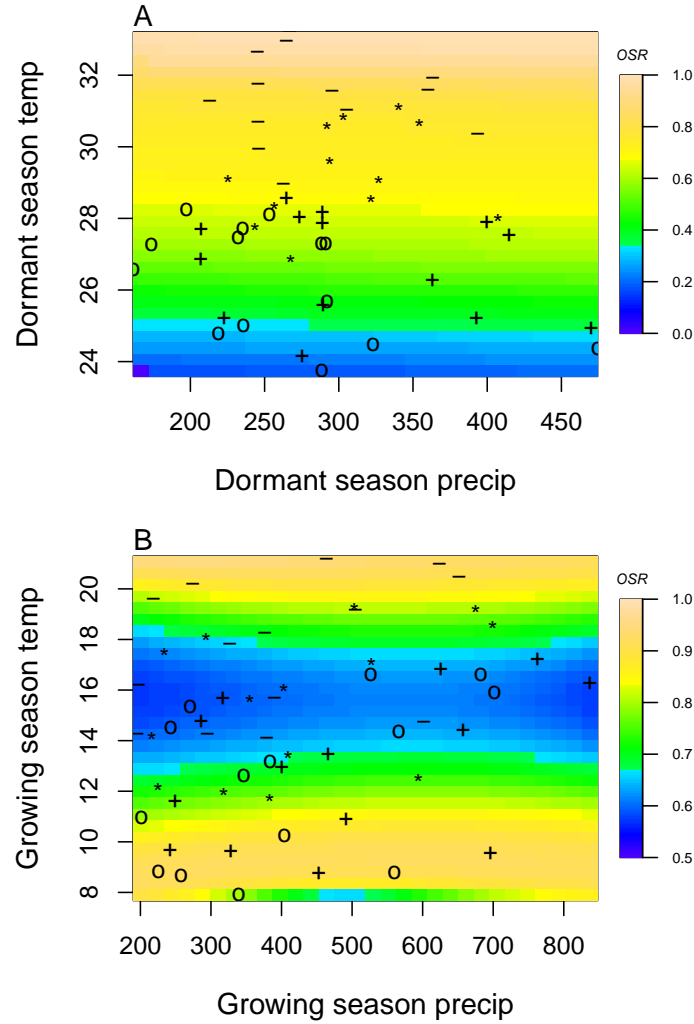


Figure S-16: A two-dimensional representation of the Operational Sex Ratio (OSR) over time (past, present and future climate conditions). OSR represents the proportion of females. Contours show predicted values of OSR conditional on precipitation and temperature of the dormant and growing season. Operational Sex Ratio during the dormant season for the two sex model (A), Operational Sex Ratio during the growing season for the two sex model (B). “**o**”: Past, “**+**”: Current, “*****”: RCP 4.5, “**-**”: RCP 8.5.

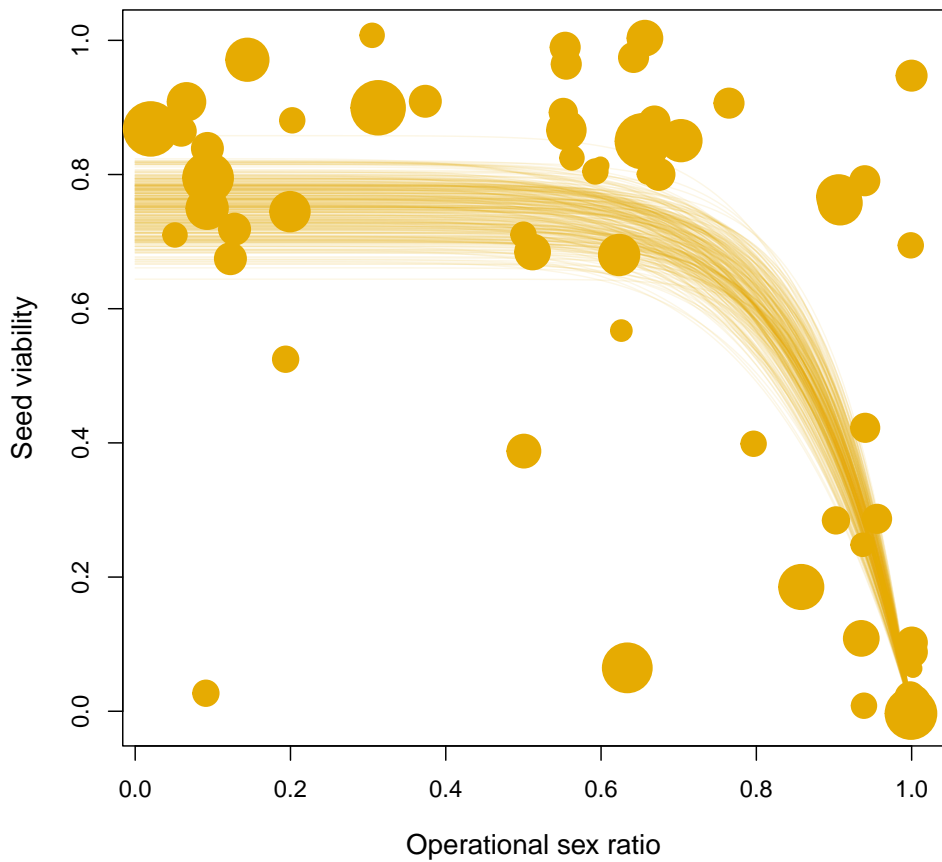


Figure S-17: Seed fertilization success as a function of operational sex ratio (fraction of panicles that are female) in experimental populations. Circles show data from tetrazolium assays of seed viability; circle size is proportional to the number of seeds tested (minimum: 14; maximum: 57). Lines show model predictions for 300 samples from the posterior distribution of parameter estimate

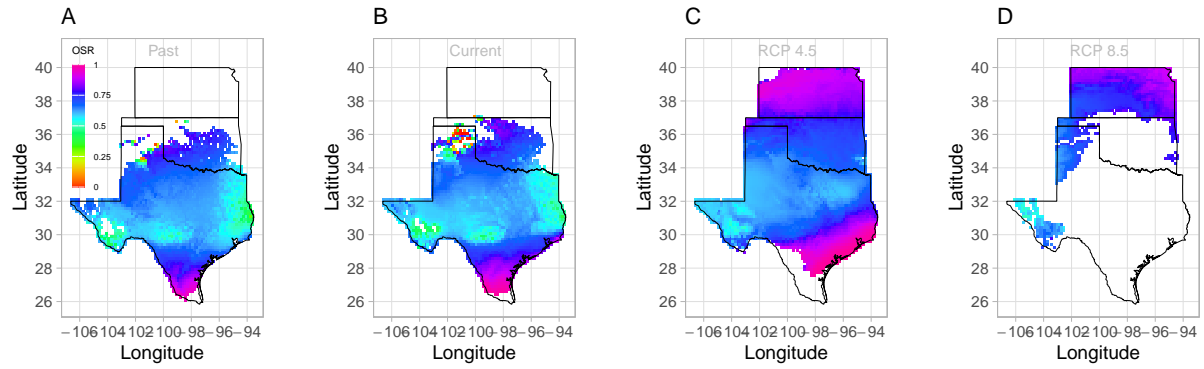


Figure S-18: Projection of Operational Sex Ratio (proportion of female panicle) over time (past, present, future) across species range. Future projections were based on the CMCC-CM model.

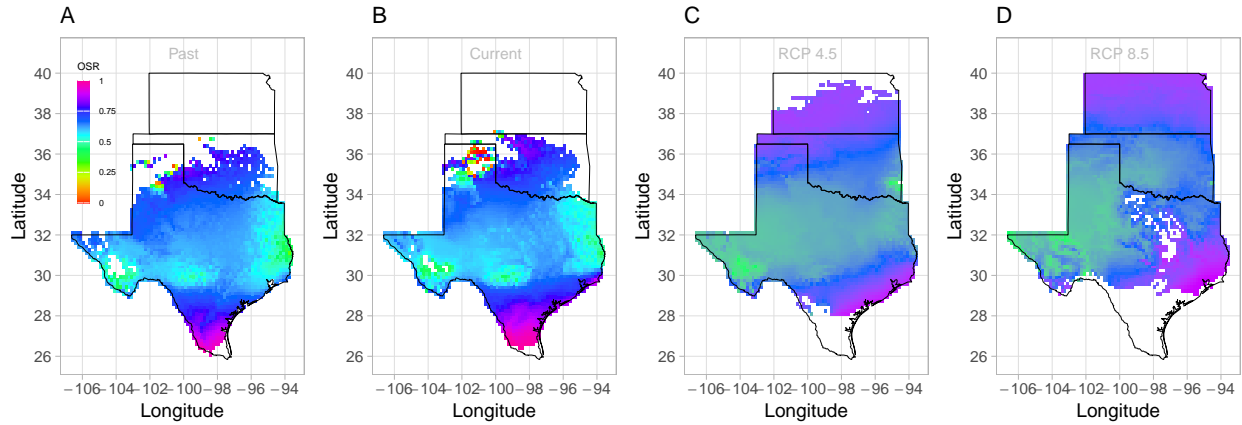


Figure S-19: Projection of in Operational Sex Ratio (proportion of female panicle) over time (past, present, future) across species range. Future projections were based on the CES model.

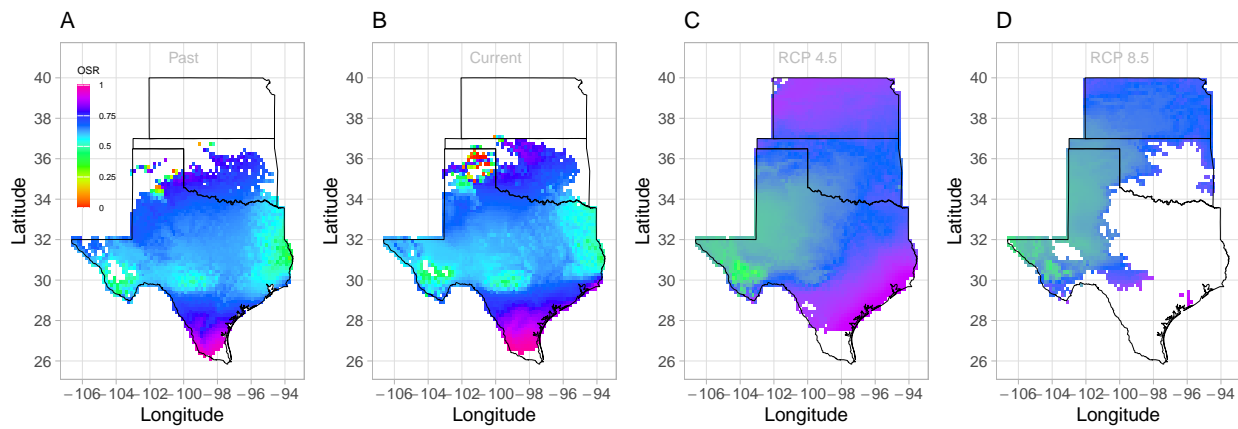


Figure S-20: Projection of Operational Sex Ratio (proportion of female panicle) over time (past, present, future) across species range. Future projections were based on the MIROC model.

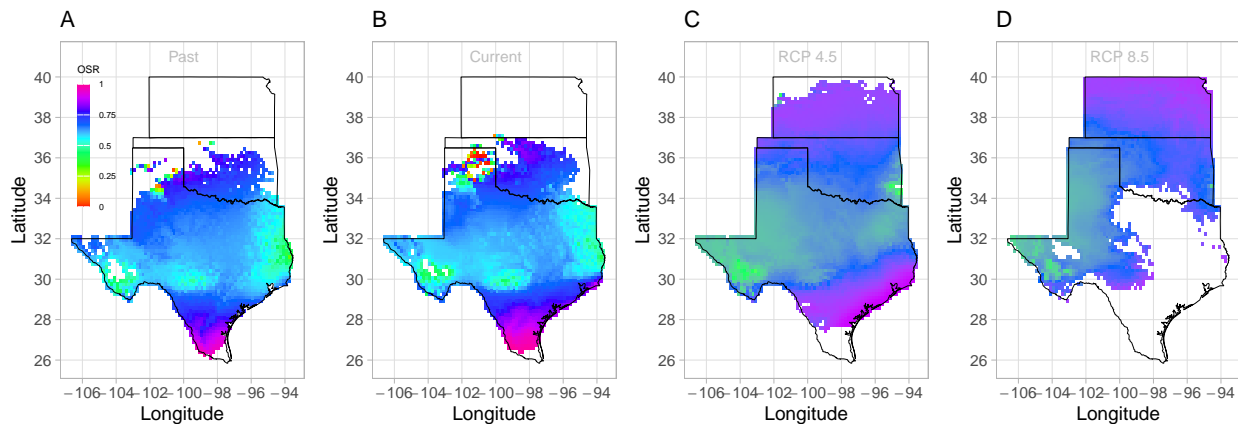


Figure S-21: Projection of Operational Sex Ratio (proportion of female panicle) over time (past, present, future) across species range. Future projections were based on the ACCESS model. The mean sex ratio for each time period is shown as vertical dashed line.

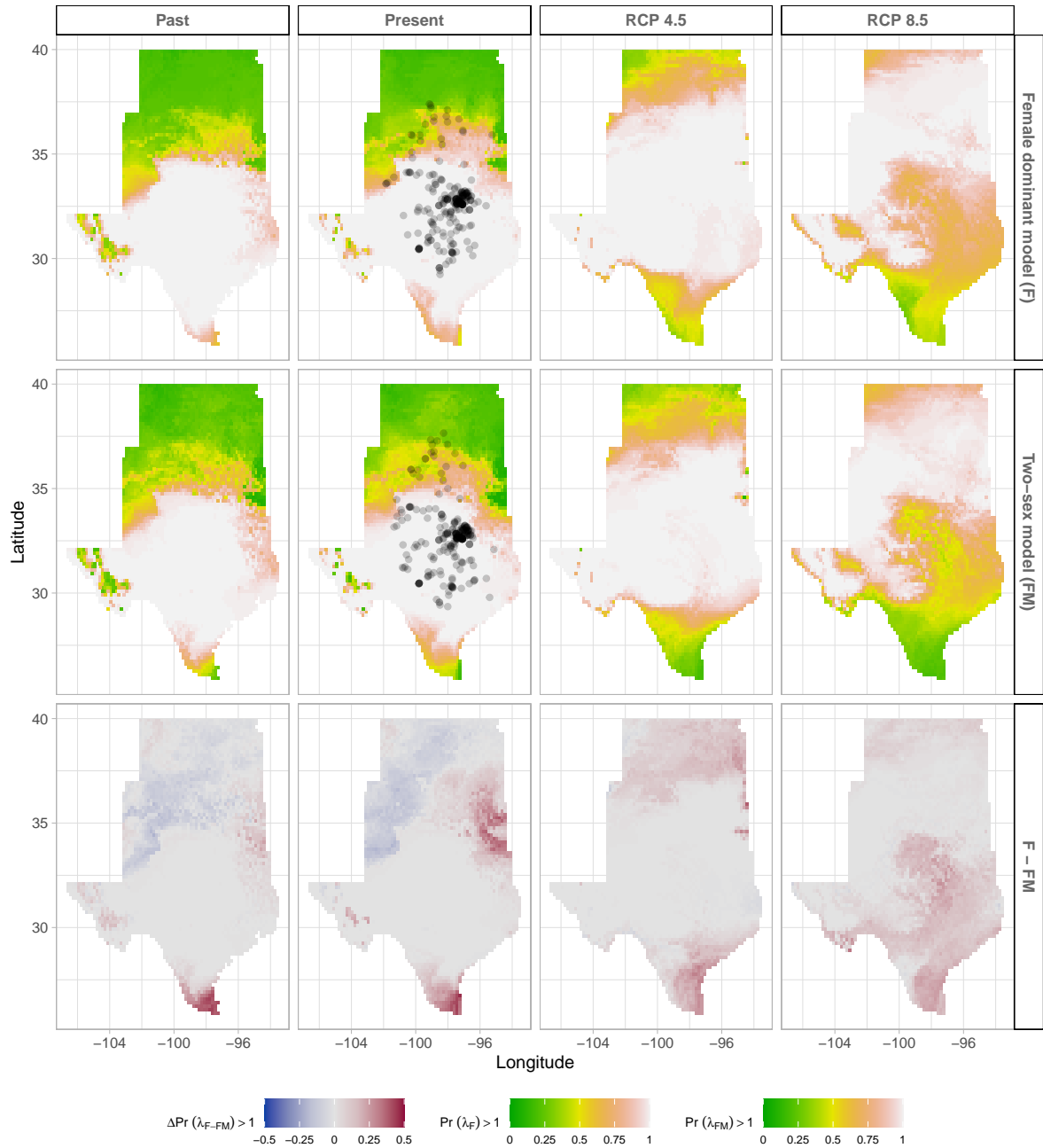


Figure S-22: Climate change favors range shift toward the North edge of the current range. (A) Past, (B) Current, (C and D) Future predicted range shift based on the predicted probabilities of self- sustaining populations, $\Pr(\lambda > 1)$, using the two-sex model that incorporates sex- specific demographic responses to climate with sex ratio dependent seed fertilization. (E) Past, (F) Current, (G and H) Future predicted range shift based on the predicted probabilities of self- sustaining populations, $\Pr(\lambda > 1)$, using the female dominant model. Future projections were based on the CESM1-BGC model. The black dots on panel B and F indicate all known presence points collected from GBIF from 1990 to 2019, which corresponds to the current condition in our prediction. The occurrences of GBIFs are distributed in with higher population fitness habitat $\Pr(\lambda > 1)$, confirming that our study approach can reasonably predict range shifts.

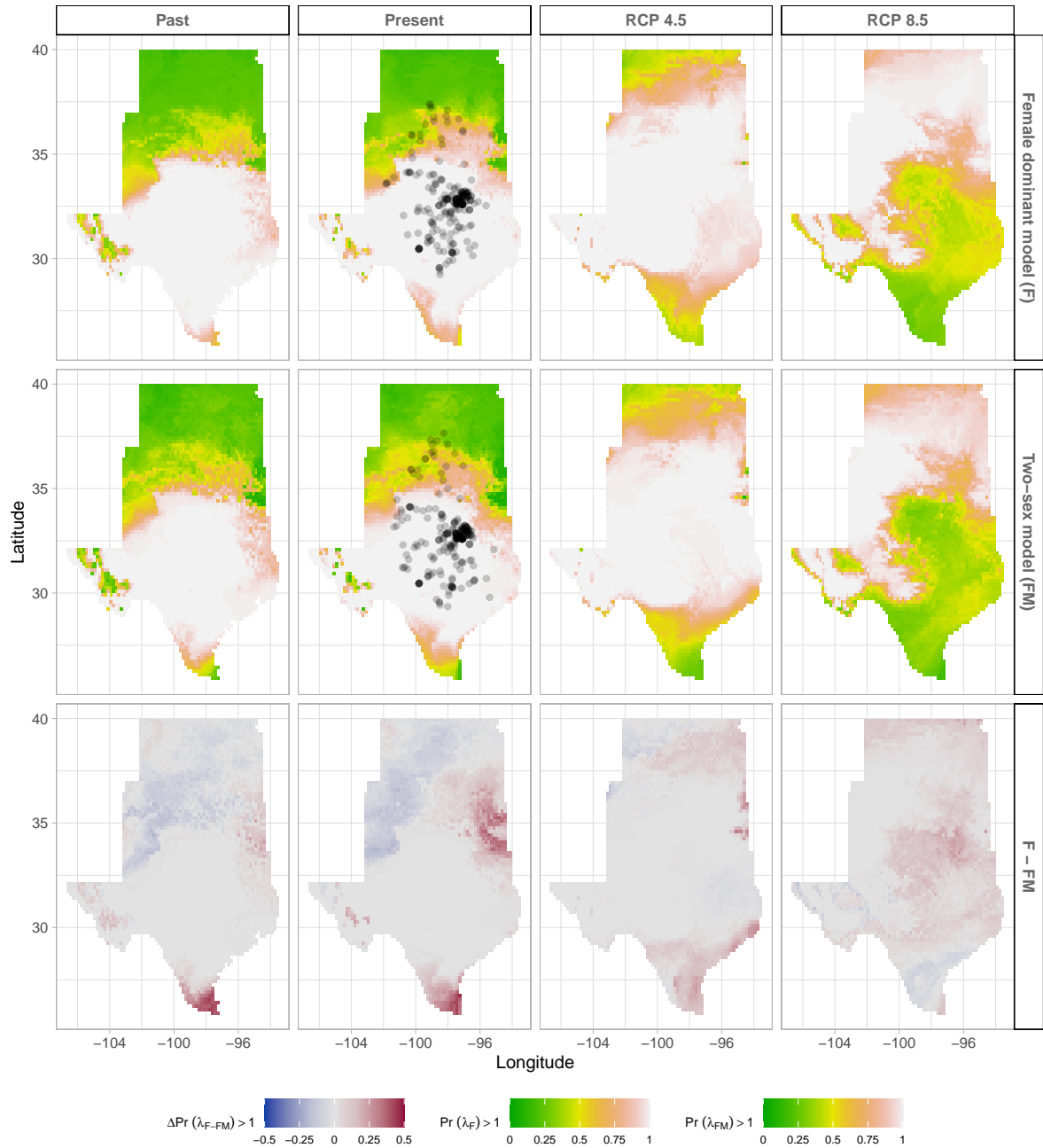


Figure S-23: Climate change favors range shift toward the North edge of the current range. (A) Past, (B) Current, (C and D) Future predicted range shift based on the predicted probabilities of self-sustaining populations, $\text{Pr}(\lambda > 1)$, using the two-sex model that incorporates sex-specific demographic responses to climate with sex ratio dependent seed fertilization. (E) Past, (F) Current, (G and H) Future predicted range shift based on the predicted probabilities of self-sustaining populations, $\text{Pr}(\lambda > 1)$, using the female dominant model. Future projections were based on the ACCESS model. The black dots on panel B and F indicate all known presence points collected from GBIF from 1990 to 2019, which corresponds to the current condition in our prediction. The occurrences of GBIFs are distributed in with higher population fitness habitat $\text{Pr}(\lambda > 1)$, confirming that our study approach can reasonably predict range shifts.

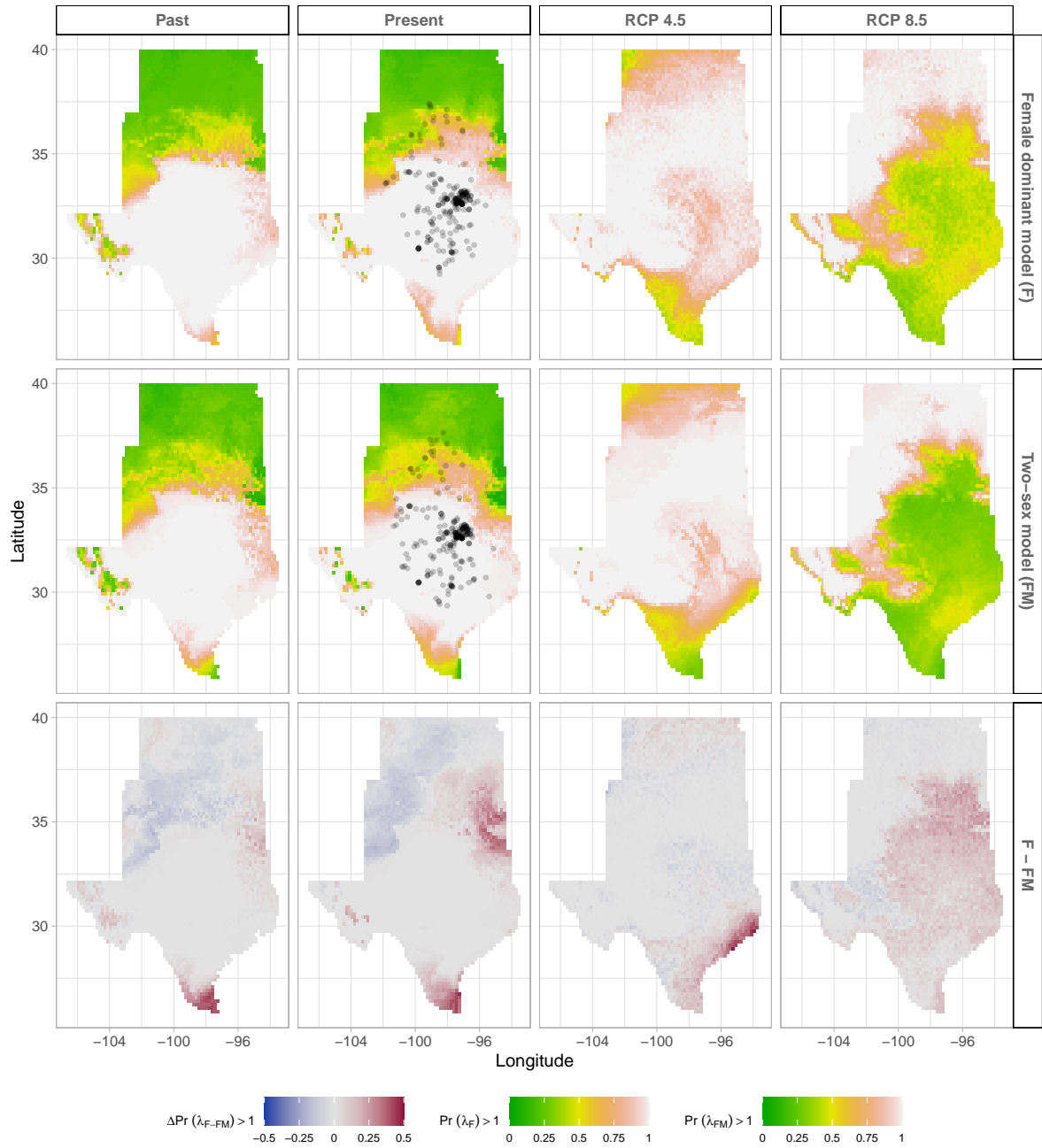


Figure S-24: Climate change favors range shift toward the North edge of the current range. (A) Past, (B) Current, (C and D) Future predicted range shift based on the predicted probabilities of self- sustaining populations, $\text{Pr}(\lambda > 1)$, using the two-sex model that incorporates sex- specific demographic responses to climate with sex ratio dependent seed fertilization. (E) Past, (F) Current, (G and H) Future predicted range shift based on the predicted probabilities of self- sustaining populations, $\text{Pr}(\lambda > 1)$, using the female dominant model. Future projections were based on the MIROC5 model. The black dots on panel B and F indicate all known presence points collected from GBIF from 1990 to 2019, which corresponds to the current condition in our prediction. The occurrences of GBIFs are distributed in with higher population fitness habitat $\text{Pr}(\lambda > 1)$, confirming that our study approach can reasonably predict range shifts.

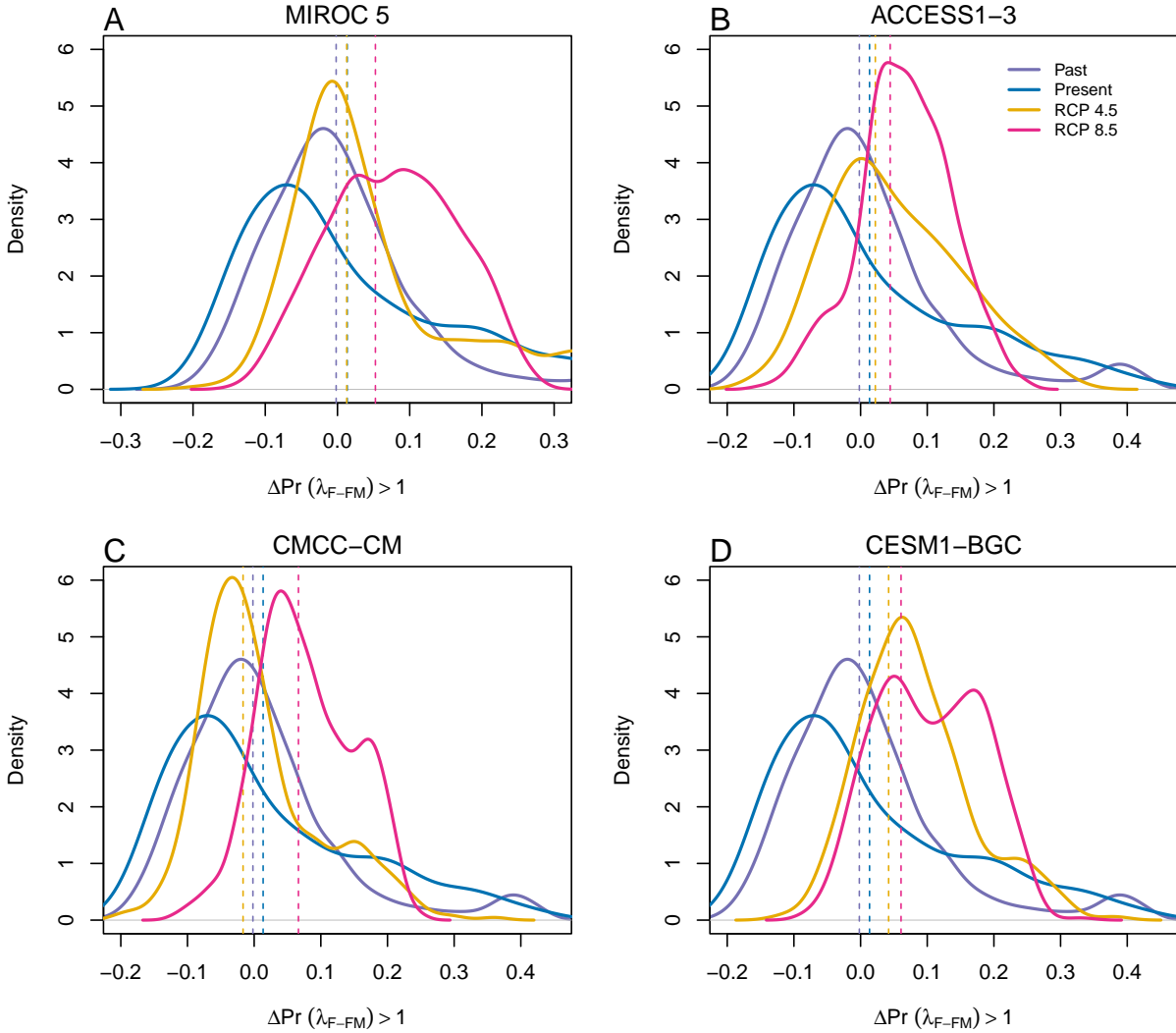


Figure S-25: Assessment of the statistical difference between the two-sex models and the female dominant model across and beyond species range for 4 GCMs. The means for each model are shown as vertical dashed lines.

685 S.2 Supporting Methods

686 S.2.1 Sex-specific demographic responses to climatic variation across 687 common garden sites

688 Vital rate models were fit with the same linear predictors for the expected value (μ) (Eq.S.1): All
689 vital rates were fit with second-degree polynomial functions to accommodate the possibility
690 of hump-shaped relationships (reduced demographic performance at both extremes). We
691 also included two-way interactions between sex and each climate driver and between
692 temperature and precipitation within each season, and a three-way interaction between sex,

693 temperature, and precipitation within each season. We modeled survival and flowering data
 694 with a Bernoulli distribution and the growth (tiller number) with a zero-truncated Poisson
 695 inverse Gaussian distribution. Fertility (panicle count conditional on flowering) was modeled
 696 as zero-truncated negative binomial. We used generic, weakly informative priors to fit
 697 coefficients for survival, growth, flowering models ($\beta \sim N(0, 1.5)$) and random effect variances
 698 ($\sigma \sim Gamma(\gamma(0.1, 0.1))$). We fit fertility model with also weakly informative priors for
 699 coefficients ($\beta \sim N(0, 0.15)$). Different priors were used for fertility because the panicle model
 700 has a large number of parameters relative to the amount of available data (subset of our data)
 701 and because these specific priors help prevent the model from overfitting. Each vital rate also
 702 includes normally distributed random effects for block-to-block variation ($\phi \sim N(0, \sigma_{block})$),
 703 site to site variation ($\nu \sim N(0, \sigma_{site})$), and source-to-source variation that is related to the
 704 genetic provenance of the transplants used to establish the common garden ($\rho \sim N(0, \sigma_{source})$).

$$\begin{aligned}
 \mu = & \beta_0 + \beta_1 size + \beta_2 sex + \beta_3 pptgrow + \beta_4 pptdorm + \beta_5 tempgrow + \beta_6 tempdorm \\
 & + \beta_7 pptgrow * sex + \beta_8 pptdorm * sex + \beta_9 tempgrow * sex + \beta_{10} tempdorm * sex \\
 & + \beta_{11} size * sex + \beta_{12} pptgrow * tempgrow + \beta_{13} pptdorm * tempdorm \\
 & + \beta_{14} pptgrow * tempgrow * sex + \beta_{15} pptdorm * tempdorm * sex + \beta_{16} pptgrow^2 \\
 & + \beta_{17} pptdorm^2 + \beta_{18} tempgrow^2 + \beta_{19} tempdorm^2 + \beta_{20} pptgrow^2 * sex \\
 & + \beta_{21} pptdorm^2 * sex + \beta_{22} tempgrow^2 * sex + \beta_{23} tempdorm^2 * sex + \phi + \rho + \nu
 \end{aligned} \tag{S.1}$$

705 where β_0 is the grand mean intercept, β_1 is the size dependent slopes. *size* was on a natural
 706 logarithm scale. $\beta_2 \dots \beta_{13}$ represent the climate dependent slopes. $\beta_{14} \dots \beta_{23}$ represent the sex-
 707 climate interaction slopes. *pptgrow* is the precipitation of the growing season, *tempgrow* is
 708 the temperature of the growing season, *pptdorm* is the precipitation of the dormant season,
 709 *tempdorm* is the temperature of the dormant season.

711 S.2.2 Sex ratio responses to climatic variation across common garden sites

712 To understand the impact of climatic variation across common garden sites on sex ratio, OSR
 713 and SR models using the same linear predictors for the expected value (ν)(Eq.S.2):

$$\begin{aligned}
 \nu = & \omega_0 + \omega_1 pptgrow + \omega_2 pptdorm + \omega_3 tempgrow + \omega_4 tempdorm + \\
 & \omega_5 pptgrow^2 + \omega_6 pptdorm^2 + \omega_7 tempgrow^2 + \omega_8 tempdorm^2 + \epsilon
 \end{aligned} \tag{S.2}$$

715 where OSR is the proportion of panicles that were female or proportion of female individuals
716 in the experimental populations, c is the climate. ω_0 is the intercept, $\omega_1, \dots, \omega_8$ are the climate
717 dependent slopes. ϵ is error term.

718 We modeled the OSR and SR data with a Bernoulli distribution and used non informative
719 priors for each coefficient ($\omega \sim N(0, 100)$).

720 S.2.3 Sex ratio experiment

721 To estimate the probability of seed viability, the germination rate and the effect of sex-ratio
722 variation on female reproductive success, we conducted a sex-ratio experiment at one site
723 near the center of the range to estimate the effect of sex-ratio variation on female reproductive
724 success. The details of the experiment are provided in Compagnoni et al. (2017) and Miller
725 and Compagnoni (2022b). Here we provide a summary of the experiment. We established
726 124 experimental populations in plots measuring $0.4 \times 0.4\text{m}$ and separated by at least 15m
727 from each other. We varied population density (1-48 plants/plot) and sex ratio (0%-100%
728 female) across the experimental populations, and we replicated 34 combinations of density
729 and sex ratio. We collected panicles from a subset of females in each plot and recorded the
730 number of seeds in each panicle. We assessed reproductive success (seeds fertilized) using
731 greenhouse-based germination and trazolium-based seed viability assays. Seed viability was
732 modeled with a binomial distribution where the probability of viability (v) was given by:

$$733 v = v_0 * (1 - OSR^\alpha) \quad (\text{S.3})$$

734 where OSR is the proportion of panicles that were female in the experimental populations.
735 α is the parameter that control for how viability declines with increasing female bias. Further,
736 germination rate was modeled using a binomial distribution to model the germination
737 data from greenhouse trials. Given that germination was conditional on seed viability, the
738 probability of success was given by the product $v * g$, where v is a function of OSR (Eq. S.3)
739 and g is assumed to be constant.